Development and Characterization of Nitazoxanide and Quercetin Co-loaded Nanotransfersomal Gel for Topical Treatment of Cutaneous Leishmaniasis

M.Phil Thesis

by

SIDRA BASHIR

Department of Pharmacy
Faculty of Biological Sciences
Quaid-i-Azam University
Islamabad, Pakistan
2022

Development and Characterization of Nitazoxanide and Quercetin Co-loaded Nanotransfersomal Gel for Topical Treatment of Cutaneous Leishmaniasis

Thesis Submitted by

SIDRA BASHIR

Registration No. 02332013001
to
Department of Pharmacy,

In Partial Fulfillment of the Requirements for the

Degree of

Master of Philosophy

in

Pharmacy (Pharmaceutics)

Department of Pharmacy
Faculty of Biological Sciences
Quaid-i-Azam University
Islamabad, Pakistan
2022

AUTHOR'S DECLARATION

I, Sidra Bashir, hereby declare that the thesis titled **"Development and Characterization of Nitazoxanide and Quercetin Co-loaded Nanotransfersomal Gel for Topical Treatment of Cutaneous Leishmaniasis"** submitted at Department of Pharmacy, Faculty of Biological Sciences, Quaid-i-Azam University Islamabad for the award of degree of Master of Philosophy in Pharmacy (Pharmaceutics) is the result of research work carried out by me I further declare that the results presented in this thesis have not been submitted for the award of any other degree from this University or anywhere else in the country/world and the University has the rights to withdraw my M. Phil degree, if my statement is found in correct any time, even after my graduation.

_____

SIDRA BASHIR

DATE: _____

PLAGIARISM UNDERTAKING

I, Sidra Bashir, solemnly declare that research work presented in the thesis titled **"Development and Characterization of Nitazoxanide and Quercetin Co-loaded Nanotransfersomal Gel for Topical Treatment of Cutaneous Leishmaniasis"** is solely my research work with no significant contribution from any other person. Small contribution/help wherever taken has been duly acknowledged and that complete thesis has been written by me. I understand zero tolerance policy of Quaid-i-Azam University, Islamabad and HEC towards plagiarism. Therefore, I as an author of the above titled dissertation declare that no portion of my thesis is plagiarized, and every material used as reference is properly referred/cited. I undertake that if I am found guilty of committing any formal plagiarism in the above titled thesis even after award of M. Phil degree, the University reserves the right to withdraw/revoke my M. Phil degree and that HEC and University has the right to publish my name on the HEC/University Website on which names of those students are placed who submitted plagiarized thesis.

_____

SIDRA BASHIR

APPROVAL CERTIFICATE

This is to certify that dissertation titled **"Development and Characterization of Nitazoxanide and Quercetin Co-loaded Nanotransfersomal Gel for Topical Treatment of Cutaneous Leishmaniasis"** submitted by **Sidra Bashir** to the Department of Pharmacy, Faculty of Biological Sciences, Quaid-i-Azam University Islamabad, Pakistan, is accepted in its present form as it is satisfying the dissertation requirements for the Degree of Master of Philosophy in **Pharmacy (Pharmaceutics).**

Supervisor

_____

Prof. Dr. Gul Majid Khan
Professor,
Department of Pharmacy,
Quaid-i-Azam University
Islamabad, Pakistan.

External Examiner

_____

Name
Designation
Department of Pharmacy
University

Chairman

_____

Prof. Dr. Ihsan-Ul-Haq
Chairman
Department of Pharmacy,
Quaid-i-Azam University
Islamabad, Pakistan

Dated: _____

Dedicated to my Grand Parents and my Family for their unconditional love and support

TABLE OF CONTENTS

Acknowledgement……..……. i

List of Tables……...……...……... ii

List of Figures…….…… ….…….…iii

List of Abbreviations……...…….……..v

Abstract……...…….……..vii

1. INTRODUCTION……. 1

1.1. Leishmaniasis: A Tropical Neglected Disease 1

1.2. Cutaneous Leishmaniasis (CL) 1

1.1.1. Incidence, prevalence, and parasite transmission of CL..... 2

1.2.2. Clinical manifestation and diagnosis of CL..... 3

1.2.3. Available therapies for CL..... 4

1.2.4. Problems with current therapies of CL..... 4

1.3. Quercetin a Natural Flavonoid as Anti-leishmanial Agent 5

1.3.1. Physicochemical properties of QUR 5

1.3.2. QUR anti-leishmanial mechanism of action 6

1.3.3. Rational for QUR selection..... 6

1.4. Antiparasitic Drugs as Anti-leishmanial Agents..... 7

1.4.1. Nitazoxanide (NTZ) 7

1.4.2. Physicochemical properties of NTZ..... 8

1.4.3. Pharmacokinetics and pharmacodynamics of NTZ..... 8

1.4.4. Rational for NTZ selection 9

1.5. Transferosomes as Topical Drug Delivery System for CL 10

1.6. Different Preparation Methods of Transferosomes.....10

1.6.1. Thin film hydration method.....10

1.6.2. Vortexing sonication method.....11

1.6.3. Modified hand shaking method.....11

1.6.4. Suspension homogenization technique.....11

1.6.5. Centrifugation method.....12

1.6.6. Reverse phase evaporation technique.....12

1.6.7. Ethanol injection method.....12

1.7. Rationale of Study..... ……13

1.8. Aim and Objectives……...13

1.8.1. Aim.....13

1.8.2. Objectives 13

2. MATERIALS AND METHODS.....14

2.1. Materials 14

2.1.1. Chemicals and reagents 14

2.1.2. Apparatus and equipment 14

2.1.3. Animals and parasites 14

2.2. Methods 15

2.2.1. Preparation of NTZ-QUR co-loaded NT 15

2.2.2. Preparation of NTZ-QUR co-loaded NT gel (NTZ-QUR-NTG).....16

2.2.2.1. Preparation of acetic acid solution.....16

2.2.2.2. Chitosan gel preparation 16

2.3. Characterization 16

2.3.1. Characterization of NTZ-QUR co-loaded NT 16

2.3.1.1. Particle size, PDI, ZP of NTZ-QUR-NT 16

2.3.1.2. Transmission electron microscopy (TEM).....17

2.3.1.3. Fourier-transform infrared spectroscopy (FTIR).....17

2.3.1.4. Deformability index of NTZ-QUR-NT 17

2.3.2. Characterization of NTZ-QUR-NTG 18

2.3.2.1. Organoleptic evaluation and pH measurement.....18

2.3.2.2. Rheology.....18

2.3.2.3. Drug content.....18

2.3.2.4. Spreadability 18

2.3.3. Stability study.....18

2.3.4. In-vitro drug release and kinetic study 19

2.3.5. Ex-vivo skin permeation and deposition study 19

2.3.6. Skin structure evaluation after treatment 20

2.3.7. Skin irritation study and histopathological study 20

2.3.8. Qualitative macrophage uptake study.....20

2.3.9. Quantitative macrophage uptake study.....21

2.3.10. Cell viability and toxicity assay 21

2.3.11. In-vitro anti-leishmanial activity analysis against *L. tropica*.....22

2.3.12. Determination of combination index 22

2.4. Statistical Analysis 22

3. RESULTS..... 24

3.1. Standard Curve of NTZ and QUR 24
3.2. Calibration Curves of NTZ at pH 5.5 and 7.4 25
3.3. Calibration Curve of QUR at pH 5.5 and 7.4 25
3.4. Optimization of NTZ-QUR-NT 26
3.4.1. Effect of independent factors on particle size 29
3.4.2. Effect of independent factors on PDI……..……..29
3.4.3. Effect of independent factors on ZP 30
3.4.4. Effect of independent factors on %EE of NTZ and QUR. 30
3.5. TEM Analysis of NTZ-QUR-NT 32
3.7. FTIR Analysis to Assess the Compatibility of Excipients with Drugs 33
3.8. NTZ-QUR-NTG Physicochemical Characterization 34
3.9. Stability Studies 36
3.10. In-vitro Release Study of NTZ and QUR at pH 5.5 37
3.11. In-vitro Release Study of NTZ and QUR at pH 7.4 37
3.12. Release Kinetic Study.....38
3.13. Ex-vivo Skin Permeation and Deposition Studies 40
3.14. Skin Structure Evaluation After Treatment 41
3.15. Skin Irritation and Histopathology Study 42
3.16. Qualitative Macrophage Uptake Study.....43
3.17. Quantitative Macrophage Uptake Study.....44
3.18. Cell Viability and Toxicity Assay 44
3.19. In-vitro Anti-leishmanial Activity Analysis Against *L. tropica* 45
3.20. Determination of Combination Index (CI) 46
4. DISCUSSION…….....47
CONCLUSIONS…… 52
FUTURE PROSPECTIVES. 53
REFERENCES……. 54

Acknowledgement

All the praises and thanks to **Almighty Allah** who bestowed His innumerable blessings upon mankind, one of which is knowledge a distinction for mankind. I offer my gratitude to the **Holy Prophet Muhammad** صلی. ہ علیہ وسلم who preached us to seek knowledge for the betterment of mankind in particular and other creatures in general.

This dissertation is the end of my journey in obtaining my M. Phil degree. This dissertation has been kept on track and seen through to completion with the support and encouragement of numerous people including my all teachers, friends, colleagues, and various institutions.

At this moment of accomplishment, first I pay homage to my supervisors **Prof. Dr. Gul Majid Khan and Co supervisor Dr. Fakhar Ud Din.** This work would have not been possible without his guidance, support, and encouragement. Under their guidance successfully overcame many difficulties and learned a lot. I am very much thankful for their valuable advice, constructive criticism, and his extensive discussions around my work.

I am also extremely indebted to **Dr. Ihsan-Ul-Haq** (Chairman), for providing necessary infrastructure and resources to accomplish my research work. I am also thankful to Dr. Ihsan ul Haq for his support and guidance during this journey. It's my pleasure to acknowledge all the faculty members of department of Pharmacy, QAU for suggestions and constant moral support.

I am indebted to my all colleagues especially Kanwal Shabbir, Sibgha Batool, Muhammad Moneeb, Zakir Ali, Sara and Kainat for providing a stimulating and fun filled environment and many rounds of discussions in lab(s) with them helped me.

I would also like to extend warm thanks to all administrative staff, laboratory staff and collaborators at QAU for support and assistance in completing my work Last but not least, I would like to pay high regards to my, mother, mamo, brothers, sister Saba Bashir and friends Maryam Rasool, Ayesha Abbasi for their prayers, sincere encouragement.

Sidra Bashir

List of Tables

Table	Title	Page No.
1.1	Physicochemical properties of QUR	05
1.2	Physicochemical properties of NTZ	08
3.1	At different concentrations absorbances values of NTZ	24
3.2	At different concentrations absorbances values of QUR	24
3.3	Absorbance values of NTZ at different concentrations at pH 5.5 and 7.4	25
3.4	Absorbance values of NTZ at different concentrations at pH 5.5 and 7.4	25
3.5	Optimization table of NTZ-QUR-NT	28
3.6	Regression analysis of BBD for all responses	29
3.7	Characterization of NTZ-QUR-NTG	35
3.8	Stability data of NTZ-QUR-NT	36
3.9	Stability data of NTZ-QUR-NTG	36
3.10	R^2 values of all kinetic models	39
3.11	Skin permeation parameters of NTZ and QUR	41
3.12	Draize scoring data for skin irritation test	43
3.13	Quantitative data of uptake of NTZ and QUR by macrophages	44

List of Figures

Figure	Title	Page No.
1.1	Quercetin anti-leishmanial mechanism of action	07
1.2	Anti-leishmanial mechanism of Nitazoxanide	09
2.1	Preparation method of NTZ-QUR-NT via thin film hydration method	15
2.2	Preparation method of NTZ-QUR-NTG	16
3.1	Standard curve of NTZ and QUR	24
3.2	Calibration curve of NTZ at pH 5.5 (A) and 7.4 (B	25
3.3	Calibration curve of QUR at pH 5.5 (C) and 7.4 (D	26
3.4	Prepared formulations of NTZ-QUR-NT	26
3.5	Particle size and PDI of the optimized formulation	27
3.6	ZP of the optimized formulation	27
3.7	3D response surface graph showing effect of lipid, surfactant and QUR on particle size of the NTZ-QUR NT	31
3.8	3D response surface graph showing effect of lipid, surfactant and QUR on PDI of the NTZ-QUR NT	31
3.9	3D response surface graph showing effect of lipid, surfactant and QUR on ZP of the NTZ-QUR NT	31
3.10	3D response surface graph showing effect of lipid, surfactant and QUR on %EE of QUR	32

3.11	3D response surface graph showing effect of lipid, surfactant and QUR on %EE of NTZ	32
3.12	TEM image of the optimized formulation (NT-3)	33
3.13	FTIR analysis of NTZ, QUR, PL90G, PM and NTZ-QUR-NT	34
3.14	S	35
3.15	Graphical presentation of the effect of shear rate on viscosity of NTZ-QUR-NTG	35
3.16	In-vitro release of NTZ at pH 5.5 (A), In-vitro release of QUR at pH 5.5 (B), In- vitro release of NTZ at pH 7.4 (C), In-vitro release of QUR at pH7.4 (D).	38
3.17	Korsmeyer and Peppas model for NTZ release from NTZ-QUR-NT (A), Higuchi model from NTZ-QUR-NTG (B), Korsmeyer and Peppas model for QUR release from NTZ-QUR-NT (C), Higuchi model from NTZ-QUR-NTG (D)	39
3.18	Ex-vivo permeation of NTZ (A), Ex-vivo permeation of QUR (B)	41
3.19	Skin deposition of NTZ (A) and QUR (B)	41
3.20	FTIR analysis of the NTZ-QUR-NTG treated skin and its comparison with normal skin	42
3.21	Normal skin (A), 0.8% Formalin treated skin (B), NTZ-QUR-NTG treated skin (C)	43
3.22	Macrophage uptake study: Rhodamine loaded NT treated macrophages (A), Rhodamine solution treated macrophages (B)	44
3.23	Cell viability assay of the NTZ-QUR-NT and NTZ-QUR dispersion	45

List of Abbreviations

Abbreviations	Description
BBD	Box-Behnken design
CL	Cutaneous leishmaniasis
CI	Combination index
CC_{50}	Half maximal toxic concentration
DI	Deformability index
EE	Entrapment efficiency
ER	Enhancement ratio
FBS	Fetal bovine serum
FTIR	Fourier transform infrared microscopy
g/mol	Gram per mole
hr	Hour
hrs	Hours
IC_{50}	Half maximal inhibitory concentration
Jss	Flux
Kp	Permeability coefficient
mg	Milligram
mV	Millivolt
µl	Microliter
nm	Nanometer
NTZ	Nitazoxanide
NT	Nanotransfersomes
NTG	Nanotransfersomal gel
NTZ-QUR-NT	Nitazoxanide and quercetin co-loaded nanotransfersomes
NTZ-QUR-NTG	Nitazoxanide and quercetin co-loaded nanotransfersomal gel
PDI	Polydispersity index
PM's	Peritoneal macrophages
PBS	Phosphate buffer saline
QUR	Quercetin
rpm	Revolution per minute

SC	Stratum corneum
TEM	Transmission electron microscopy
TFH	Thin film hydration
VL	Visceral leishmaniasis
WHO	World health organization
ZP	Zeta potential

Abstract

Anti-leishmanial medications administered by oral and parenteral routes are less effective for treatment of cutaneous leishmaniasis (CL) and cause toxicity, hence targeted and localized drug delivery methods, are efficient way to improve drug availability for CL. The aim of study was to develop nitazoxanide and quercetin co-loaded nanotransfersomes (NTZ-QUR-NT) for topical delivery of drugs against CL. To prepare NTZ-QUR-NT thin film hydration method was used and they were statistically optimized by using Box-Behnken Design in terms of particle size, zeta potential (ZP), polydispersity index (PDI) and entrapment efficiency (EE) of both drugs. Lipid, surfactant and QUR concentrations were taken as independent variables. Transmission Electron Microscopy (TEM) analysis was performed for surface morphology and particle size assessment. Fourier-transform infrared spectroscopy (FTIR) was performed to identify any chemical interaction between components of the formulation. NTZ-QUR-NT were incorporated into 2% chitosan gel to prepare NTZ-QUR-NT gel (NTZ-QUR-NTG). In-vitro release of NTZ-QUR-NT, NTZ-QUR-NTG and NTZ, QUR dispersions were performed to check the release pattern of drugs. To evaluate the penetration behavior of NTZ-QUR-NT and NTZ-QUR-NTG as compared to NTZ and QUR gels (conventional gels), ex-vivo permeation study was performed using Franz diffusion cells. Macrophage uptake, cell viability and toxicity study were performed to investigate the macrophage targeting and potential toxic effects of NTZ-QUR-NT in comparison with NTZ-QUR dispersion. The anti-leishmanial assay was performed to evaluate the anti-leishmanial potential of NTZ-QUR-NT as compared to NTZ-QUR dispersion.

The optimized formulation indicated particle size of 210.9 ± 3.67 nm, PDI of 0.155 ± 0.009, ZP of -15.06 ± 1.48 mV and EE of NTZ and QUR 88.04 ± 0.01% and 85.14 ± 0.02%, respectively. TEM analysis of the optimized NTZ-QUR-NT showed spherical and uniform particles. No chemical interaction between components of NTZ-QUR-NT was found after Fourier-transform infrared spectroscopy (FTIR) analysis. In-vitro release of NTZ and QUR from NTZ-QUR-NT and NTZ-QUR-NTG showed more sustained behavior as compared to NTZ, QUR dispersions. Significant increase in skin permeation of NTZ and QUR was observed in case of NTZ-QUR-NT and NTZ-QUR-NTG in comparison to conventional gels. To ease the topical delivery the NTZ-QUR-NT were dispersed in 2% chitosan gel. Skin deposition studies demonstrated the better

retention profiles of drugs in case of NTZ-QUR-NT and NTZ-QUR-NTG at dermal level. In-vivo skin irritation and histopathological findings did not show any topical irritation associated with NTZ-QUR-NTG. Macrophage uptake analysis showed that NTZ-QUR-NT cell internalization was almost 10-folds higher in comparison to NTZ-QUR dispersion. It was clear from result that NTZ-QUR dispersion was distributed rather than particularly internalized by macrophage. The cytotoxicity result showed that NTZ-QUR-NT have CC_{50} value of 71.95 ± 3.32 µg/ml and NTZ-QUR dispersion have 49.77 ± 2.15 µg/ml, respectively, which indicates that NTZ-QUR-NT is safer to use as compared to NTZ-QUR dispersion. Moreover, in-vitro anti-leishmanial assay presented that NTZ-QUR-NT have IC_{50} value of 3.15 ± 0.89 µg/ml against *Leishmania tropica* promastigotes which was 6.24-times lower than NTZ-QUR dispersion. For the deep-seated infections like leishmaniasis, topical application of NTZ-QUR-NTG would be a suitable choice because of its targeted action and efficacy as evident in this study.

CHAPTER 1

INTRODUCTION

1. INTRODUCTION

1.1. Leishmaniasis: A Tropical Neglected Disease

Leishmaniasis is a parasitic infection which is common in tropical areas and being neglected for decades. It is considered to be the ninth major cause of disease amid infected individuals (Alvar *et al.*, 2012). It is caused by intracellular species of kinetoplast and protozoa from genus Leishmania and transmitted by vector sand fly of genera Phlebotomus. It is considered as disease of poor people living in developing countries and having low socioeconomic status (Sharma *et al.*, 2021). Throughout the world 98 nations are endemic with leishmania and over 350 million individuals are at risk. From localized simple lesions to the complex diffused lesions which lead to the reticuloendothelial system to clinically leishmania can be divided into three main types visceral, muco-cutaneous and cutaneous leishmania (Desjeux, 2004). These distinctive clinical presentations are ascribable to immune system response diversification among different persons against various leishmania parasite variants (Surur *et al.*, 2020).

1.2. Cutaneous Leishmaniasis (CL)

CL is a serious health concern that can result in a wide range of illnesses, from chronic degenerative diseases to self-healing infections. CL is characterized by the development of abscesses and persistent skin inflammation (Scott and Novais, 2016). Tiny nodules, plaques, and lesions that resemble ulcers can all be found on the skin's surface. *Leishmania major* (*L. major*), *Leishmania aethiopica* (*L. aethiopica*) , and *Leishmania tropica* (*L. tropica*) are the main parasites that cause CL, and sand flies are the primary vector for the parasites' propagation into humans (Bailey, 2011; Batool *et al.*, 2021). The amastigote form evolved to survive and even proliferate in challenging conditions inside the macrophage (Vannier-Santos *et al.*, 2005; Rabia *et al.*, 2020).

CL can be categorized according to geographical location and dermatological symptoms (diffuse and localized). Amastigote and promastigote are CL's two developmental stage classifications (Baileyid *et al.*, 2019). Amastigote form exists on the inside of mammalian macrophage cells, while promastigote is found in the sand fly's GIT. When a sand fly bites an infected mammal, it also absorbs macrophages and an amastigote, which develops into a promastigote in the midgut of the sand fly and matures there. The mature promastigote then proceeds in the direction of the fly's

proboscis and is now capable of infecting other healthy animals through bite (Valero and Uriarte, 2020).

Although CL is a non-lethal disease, it sometimes causes major impairment and leaves permanent skin scars. The disease is typically self-curable in between six months and a year, but the main danger is the appearance of unsightly lesions, especially when they affect the face or other conspicuous areas of the body (Alvar *et al.*, 2006).

1.2.1 Incidence, prevalence, and parasite transmission of CL

Globally, there are thought to be 0.7 to 1 million CL new cases every year. According to the 2019 Global Status report on diseases, there are 4.6 million instances with prevalent CL worldwide. Around 80% of CL cases recorded in 2020 were from Afghanistan, Brazil, Iraq, Pakistan, Iran and the Syrian Arab Republic (Hernández-bojorge et al., 2020). There are several factors that contribute to the spread of disease to new regions, but the primary ones are ecological disruption, poor socioeconomic conditions, resistance, migration, and various immune system ailments (Bamorovat *et al.*, 2018). Recent research has documented the impact of CL on Pakistan's various areas. The principal causative agent of anthroponotic CL and zoonotic CL was *L. tropica* and *L. major*, respectively, was found in the northern and western regions of Pakistan with substantial CL burdens. The main factors contributing to the spread of illness were unsanitary living circumstances, domestic animals and related waste, migration, the prevalence of pets, and outdoor sleeping practices (Khan *et al.*, 2016).

Leishmania infantum is primarily found in wild mammals like hare and dogs, and infection in humans requires either a sufficient anthroponotic or zoonotic transference to the host. In addition to the main method of transmission, which is vector transmission, the parasite can also spread by non-vector routes such as organ transplantation, blood product transfusion, and laboratory accidents, albeit transmission through these channels is seldom documented (Jamshaid *et al.*, 2021). The principal host cell for parasite replication is the macrophage, where the parasite lives and multiplies as a result of multiple morphological changes, suppression of TNF, IL-12, and iNOS, as well as an increase in the levels of IL-10, PGE2, and TGF. T-cells, which are a component of the immune system, produce signals that aid in reducing the aforementioned process and the parasite burden (Christensen *et al.*, 2018).

1.2.2. Clinical manifestation and diagnosis of CL

CL begins with the development of a papule at the site of infection, which is frequently found on exposed body parts like the face or extremities. The papule typically turns into a nodule with an ulcerogenic propensity (Abadías-Granado *et al.*, 2021). Multiple or single CL lesions are possible, and the infection may progress through the lymphatic system to cause satellite lesions, sporotrichoid lesions, and enlargement of lymph nodes (de Carvalho *et al.*, 2017).

As a diagnostic parameter physical appearance of skin lesion is used but due to the similarity between clinical manifestations of CL with cutaneous cancer, fungal infections and leprosy differential diagnosis is required (Reithinger and Dujardin, 2007). Molecular testing based on nuclear or kinetoplast DNA amplification is used to demonstrate the presence of Leishmania amastigotes in clinical specimens to make the diagnosis of leishmaniasis. Amastigotes are spherical, 1–4 μm in diameter, and have a distinctive rod-shaped structure called a kinetoplast. Until recently, the main methods for diagnosing CL were clinical symptoms, microscopic examination of the parasites in stained tissue or promastigote culture from tissue (Rasti *et al.*, 2016).

In many tropical areas where leishmaniasis is endemic, microscopic detection and parasite cultures are still used as the main diagnostic techniques (Marques *et al.*, 2006). The gold standard for diagnosis has historically been the cultivation of promastigotes out from infected tissues and/or the direct detection of amastigotes in microscopy smears. These methods are not sensitive, but they're quite specific for detecting leishmaniasis. Since traditional parasitological approaches are insufficiently sensitive, the use of polymerase chain reaction (PCR) test has gradually taken over as the main method for diagnosing leishmaniasis. Currently, no one laboratory method is acknowledged as the gold standard for determining leishmanial infection. A "gold standard" status for the testing of CL by PCR appears to be on the horizon as a result of recent advancements in specimen collecting, transportation, and DNA extraction techniques (Pourmohammadi *et al.*, 2010). Due to the absence of high technology instruments in health care settings of developing countries microscopic examination is most commonly use (Al-Jawabreh *et al.*, 2006).

1.2.3. Available therapies for CL

Most of the time, CL has been seen to be self-healing. However, MCL and regional lymphangitis can seriously damage tissue. Full recovery takes months to years, and during this time the patient is prone to secondary infections, permanent scarring, and function impairment. Due to the scarcity of evidence-based data, the majority of treatment decisions must be made based on expert opinions regarding the course of leishmaniasis. In comparison to several other infectious disorders, identifying the Leishmania that is causing an infection is fairly challenging (Briones Nieva *et al.*, 2021). There is still a paucity of CL treatments that are both efficient and cheap. It wasn't considered a direct threat to industrialized nations until it was free of co-infection with HIV and AIDS. The lack of chemoprophylaxis or vaccination made CL chemotherapy less effective, which made it more difficult. Unfortunately, even basic microscopy isn't really available at the level of basic services in healthcare because the majority of cases are reported in distant areas (Briones Nieva *et al.*, 2021).

There are many options for treating CL. Pentavalent antimonials, such as pentostam or, sodium stibogluconate, and Glucantime, are typically regarded as the first-choice treatment for CL (Agrahari and Mitra, 2016). Pentamidine, miltefosine, amphotericin B, paromomycin, antifungals like ketoconazole, fluconazole, and itraconazole are considered as alternate therapies (Ferreira *et al.*, 2004; Nazari-Vanani *et al.*, 2018). Similarly, heat therapy or cryotherapy, and granulocyte macrophage colony-stimulating factor are some additional treatments (Minodier and Parola, 2007).

1.2.4. Problems with current therapies of CL

Various issues are connected to the treatments that are currently available. For instance, sodium stibogluconate needs prolonged IV therapy and might cause toxicity; as a result, a longer hospital stays of up to 20 days may be required for complete treatment. Pentamidine and berbarin sulphate both cause pain and the production of scars at the injection site (Andrade-neto *et al.*, 2018). Amphotericin-B is effective against fungus and leishmanial infections, but its usage has been constrained due to toxicity and systemic adverse effects. Nephrotoxicity and unpleasant effects due to infusion are its main limiting factors (Srivastava *et al.*, 2011).

Miltefosine has been licensed for oral use in the treatment of leishmaniasis, but numerous unfavorable side effects, including gastrointestinal discomfort, hemolysis,

and nephrotoxicity, remain its main dose-limiting factors and contribute to low patient (Srivastava *et al.*, 2017). Anti-leishmanial medications are now subject to the problem of drug resistance, which is becoming more and more common (Yasinzai *et al.*, 2013). There are also no effective preventative Leishmania vaccinations, and the toxicity of the existing treatments is a problem. Finding novel treatments and developing them should be a key priority in light of these problems (Jamshaid *et al.*, 2021).

1.3. Quercetin a Natural Flavonoid as Anti-leishmanial Agent

Lack of effective immunizations and limited pharmacological alternatives for the disease emphasize the need to look for new therapeutic agents from both natural and synthetic drug pools. To overcome the problems of monotherapy like toxicity long duration of treatment, resistance emergence, combination therapy seems to be the best option (Tiwari *et al.*, 2017). Plant based medicines are good alternative as they are cheap and have low or no side effects as compared to chemotherapy (Gervazoni *et al.*, 2020). Quercetin (QUR) a natural polyphenolic compound and it is most commonly used flavonoid because of its anti-cancer, anti-inflammatory, antioxidation and antileishmanial properties (Oryan, 2015).

1.3.1. Physicochemical properties of QUR

The molecular formula of QUR is $C_{15}H_{10}O_7$ and chemical name is 3,3,4,5,7, penta-hydroxy flavone. It is less soluble in alcohols and practically insoluble in water. With low solubility it also has permeability issue due to presence of polar groups in sits structure (Maurya, 2022).

Table 1.1. Physicochemical properties of QUR.

Physical properties	Description	Reference
Appearance	Yellow orange powder	(Mussoi *et al.*, 2017)
Molecular weight	302.24 g/mol	
Melting point	316.5 ºC	
Formal charge	0	
Log P	1.82	(Rothwell *et al.*, 2005)
pKa	6.38	
Solubility	0.17-7.7 µg/ml	(Gao *et al.*, 2009)

1.3.2. QUR anti-leishmanial mechanism of action

Basically, in macrophage two enzymes are acting on arginine one is parasite arginase which leads to formation of polyamines require for parasite replication and other is macrophagal nitric oxide synthase which lead to formation of nitric oxides which causes the parasite death. QUR shows its anti-leishmanial effect by inhibiting the arginase an important enzyme for parasite proliferation. (Sousa-Batista *et al.*, 2017). It also causes the mitochondrial damage of parasite by increasing ROS level (Gervazoni *et al.*, 2020). Another study showed that it is potent activator of nuclear factor-erythroid 2 related factor 2 (Nrf2) which plays very important role for the regulation of genes that carry ARE motif like ferroportin and H-ferritin that are involved in regulation of labile iron. This labile iron is used by leishmania parasite inside the macrophage for replication and survival. But QUR act as iron chelator by using Nrf2/OH-1 to decrease the concentration of labile iron and increase the bound iron. As no labile iron will be available for parasite which lead to its death (Henrique *et al.*, 2019). **Figure 1.1** demonstrates the anti-leishmanial mechanism of QUR.

1.3.3. Rational for QUR selection

QUR showed IC_{50} value of 182.3 µg/ml for *L. tropica* promastigotes and 31.4 µM for *L. amazonensis* species promastigotes in previous studies (Mehwish *et al.*, 2019). Toxicity studies showed no rise in hepatic or renal enzymes or other side effects like anemia, nephrotoxicity in case of chemotherapy. QUR has been purposed as potential candidate in combination with other antileishmanial agents for treatment of cutaneous leishmaniasis (Sarkar *et al.*, 2002).

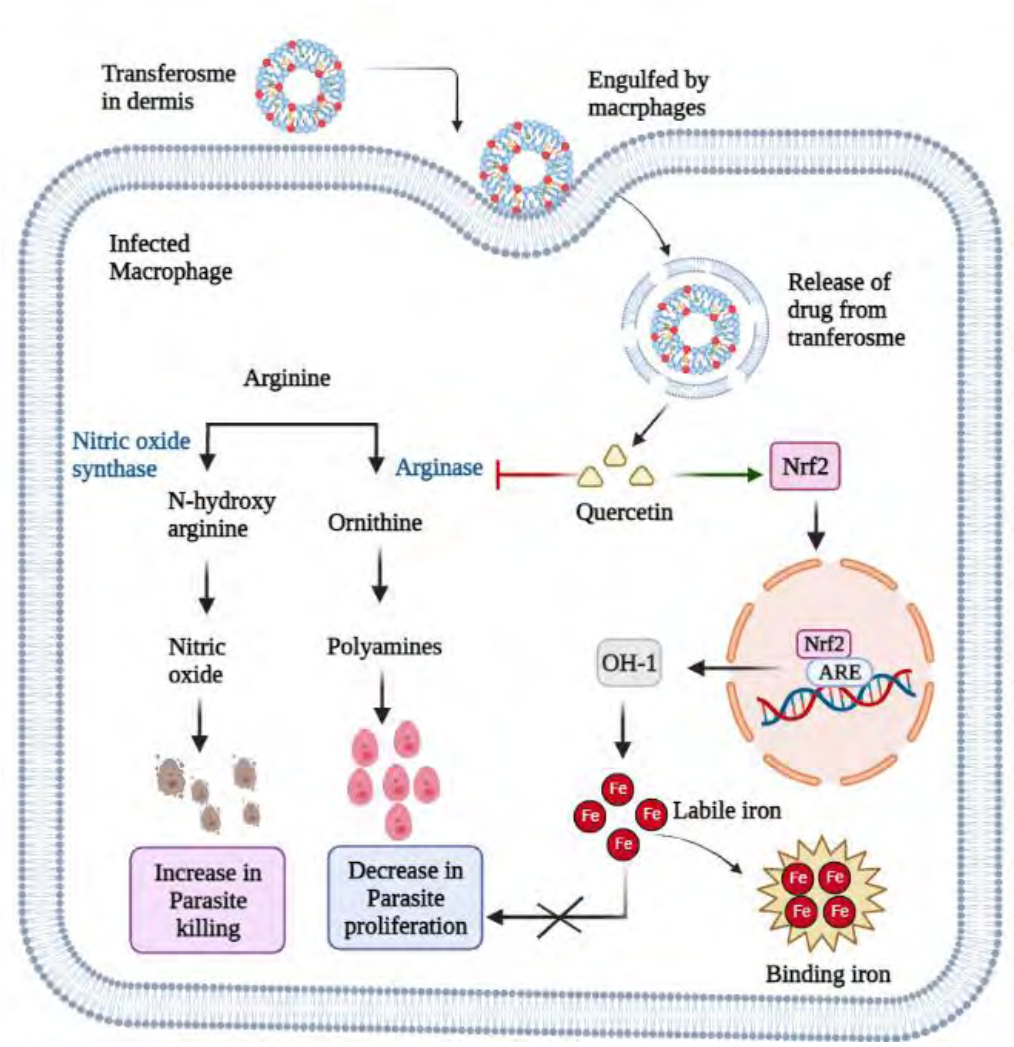

Figure 1.1A. QUR anti-leishmanial mechanism of action. Figure is designed via Biorender

1.4. Antiparasitic Drugs as Anti-leishmanial Agents

Currently, Antiparasitic drugs that cause oxidative stress like increased production of reactive oxygen species and inhibit redox enzyme are considered novel therapeutic candidate for treatment of leishmaniasis (Pal and Bandyopadhyay, 2012). As redox system plays vital role in growth and development of leishmania parasites and cope with oxidative stress. But when redox enzymes are inhibited, and oxidative stress is increased redox system fail to protect the parasite which leads to its death (Simeonov *et al.*, 2008; Pal and Bandyopadhyay, 2012).

1.4.1. Nitazoxanide (NTZ)

Its chemical name is 2-acetyloloxy-N-(5-nitro 2 thiazolyl) benzamide and it belongs to thiazolide class (Jr, 2004). It is immediately metabolized into its active form tizoxanide in human beings. Even though both nitazoxanide and its metabolite are equally potent, but it is easy to administer parent drug as compared to its metabolite because of its

lipophilic nature. Another reason is the phenolic moiety in metabolite cause irritation of gastrointestinal tract mucous membrane (Chan-Bacab *et al.*, 2009).

Earliest time nitazoxanide was used as anthelminthic for treatment of liver trematodes and intestinal nematodes in animals as reported by Jean Francois Rossignol in 1975.while in 1984 for the first time it was used for human against *taenia saginata* and *hyemenolepis nana* as cestocidal agent. In 2002, it was approved by Food and Drug Administration (FDA) in USA for treatment of cryptosporidiosis and giardiasis. Oral suspension and tablets of nitazoxanide are also available commercially as Alinia® (Lancet and Diseases, 2014).

1.4.2. Physicochemical properties of NTZ

NTZ is appeared as yellow crystalline powder that belongs to BCS class IV and insoluble in water. It is more soluble in methanol as compared to ethanol. The molecular formula of NTZ is $C_{12}H_9N_3O_5S$ and molecular weight of NTZ is 302 g/mol and its boiling and melting point is 394 ºC and 202 ºC (Firake *et al.*, 2017).

Table 1.2. Physicochemical properties of NTZ.

Physical properties	Description	Reference
Appearance	Crystalline powder	(Firake *et al.*, 2017)
Color	Yellow	
Molecular weight	307.283 g/mol	
Melting point	202 ºC	
Formal charge	0	
Log P	1.63	
Solubility	0.00755 mg/ml	(Sood *et al.*, 2020)

1.4.3. Pharmacokinetics and pharmacodynamics of NTZ

When NTZ is taken orally and reached into blood it is converted into tizoxanide which is also called as diacetyl nitazoxanide by enzyme esterase. It is highly protein bound almost 99% of this active metabolite is bound to protein and excreted with feces while one third by urine. The elimination half-life of tizoxanide is 1.8 hr. the absorption of nitazoxanide is increased with food. NTZ is a broad spectrum antiparasitic drug which shows its action by inhibiting the important enzyme pyruvate ferredoxin oxidoreductase

(PFOR) which play critical role in energy metabolism of most of parasites and bacteria. Basically, NTZ inhibit the first step by hindering the binding of pyruvate to thiamine pyrophosphate which lead to no production of ATP and eventually parasites death as illustrated in **Figure 1.2** (Anderson and Curran, 2007).

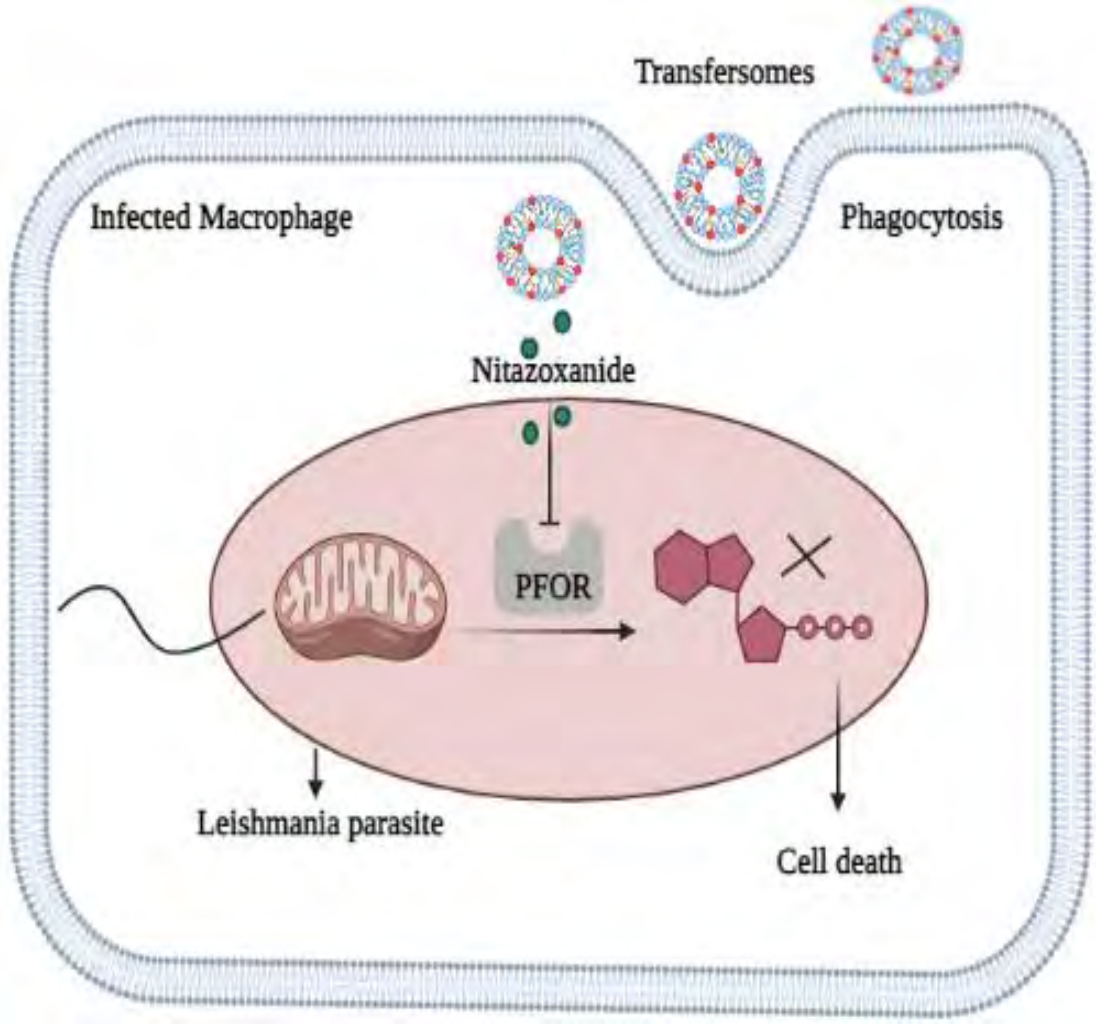

Figure 1.2. Anti-leishmanial mechanism of Nitazoxanide. Figure is created via Biorender

1.4.4. Rational for NTZ selection

In comparison to alternative treatments, nitazoxanide (NTZ) has a good side effect profile. NTZ is a more effective antiparasitic medication for leishmania than other second-line medicines that are primarily focused on bacterial or fungal species. (Gurgen *et al.*, 2011) A total of 200 µg/mL nitazoxanide inhibits the growth of > 90% of promastigotes showing activity similar to that of the reference drug amphotericin B ($P > 0.05$) alone in the in-vitro conditions (Zhang *et al.*, 2010). Recently, oral liposomes of NTZ were formulated for treatment of leishmania and results were showing better

efficacy even at very low doses as compared to conventional formulation (Gracielle *et al.*, 2020). Due to its selective action on parasites and the need to produce new treatment for leishmaniasis, it was chosen to study the effects of NTZ in combination with QUR.

1.5. Transferosomes as Topical Drug Delivery System for CL

Due to its benefits over oral or parenteral routes, World Health Organization (WHO) considers topical medication delivery systems to be the best option for treating cutaneous leishmania. Because it offers prolonged drug release, localized activity without first pass metabolism, and reduced systemic toxicity, the topical route is recommended (Agrahari and Mitra, 2016). The main issue with topical distribution is getting the desired effect into the deeper layers of the skin by penetrating through the stratum corneum. Thus, the ideal delivery method is one that can pass through the skin's layers, enter macrophages, and allow the medicine to be released intracellularly (Fernández-García *et al.*, 2020a; Rabia *et al.*, 2020).

The first-generation deformable vesicles created by Cevc, and Blume are called transferosomes. Deep penetration of vesicles into the skin has long been a contentious issue because, according to a number of studies, they are restricted to the top layers of the SC while ultra-deformable vesicles are said to cross the various skin layers as a result of the emergence of a natural hydration gradient (Cevc and Blume, 2001). The capacity to deform vesicles is advantageous for skin penetration because it lowers the risk of vesicular harm. Furthermore, when used in non-occluded settings, it utilizes a hydration gradient to aid vesicles' penetration into the deeper skin layers (Barry, 2004; Batool *et al.*, 2021).

Gels are thought to be promising delivery systems for keeping medications or nanoparticles in place where they are applied (Gao *et al.*, 2016). Gels' mucoadhesive properties also lengthen the drug's duration in the body. By incorporating NTs inside a gel matrix, it is possible for the NTs to permeate the skin for a prolonged period at the CL lesions (Dar *et al.*, 2020). The leishmanial strains are subsequently eliminated by macrophages after NTs have passed through the epidermal layers, encouraging healing (Salim *et al.*, 2020).

1.6. Different Preparation Methods of Transferosomes

1.6.1. Thin film hydration method

The term "rotary evaporation technique" is another name for this process. First, the organic phase is made by combining the lipid and edge activator with organic solvents like methanol, chloroform, etc. in a rotary flask. A dry thin film then forms on the bottom of the flask after the entire organic solvent has been evaporated using a rotary evaporator. The produced film is then hydrated with phosphate buffer for an hour in the following step. After obtaining the dispersion, nanotransfersomes are produced by sonicating and extruding the mixture via membrane filters (El Maghraby *et al.*, 2010).

1.6.2. Vortexing sonication method

All of the materials (lipid, surfactant, and drug) are combined and mixed in phosphate buffer dispersion during the vortex sonication process. Then the fluid is vortexed until transfersomes have developed a milky colored dispersion. The resulting milky dispersion is then projected through polycarbonate filters after being sonicated in a water bath for a predetermined amount of time (Sharma *et al.*, 2014).

1.6.3. Modified hand shaking method

The modified hand shaking method uses the same rotating evaporation principle. In a round bottom flask with organic solvent, surfactant, phospholipid, and hydrophobic medication added, these materials are thoroughly dissolved until a clear solution is formed. The organic solvent is then removed from the solution by hand shaking as opposed to a rotating evaporator. A high-temperature water bath should be used to submerge a round-bottom flask (for instance, 40–60 °C). After all traces of the organic solvent had been evaporated, a thin coating had formed on the bottom of the flask. The flask was held in vacuum for the entire night to remove any remaining solvent from the produced film. The resulting film is gently shaken above its phase transition temperature to hydrate it with phosphate buffer solution (Laxmi *et al.*, 2015).

1.6.4. Suspension homogenization technique

When ethanolic phospholipid solution and a specific amount of surfactant are combined, ultra- deformable transferosomes are created. After that, the produced solution is included with phosphate buffer to obtain the total lipid concentration. The finished product is then sonicated, frozen, and thawed two to three times (Apsara *et al.*, 2020).

1.6.5. Centrifugation method

In a round bottom flask, all of the ingredients (phospholipid, lipophilic drug and edge activator) are dissolved in organic solvents. After that by using a rotating evaporator vacuum at a set temperature, the organic solvent is evaporated. A film forms at the bottom of the flask after the organic solvent has been completely removed. At room temperature, phosphate buffer is used to hydrate the produced film in a centrifuge. Incorporating water-soluble drugs is possible at this stage. To create uni-lamellar vesicles, the generated multilamellar vesicles are subjected to further sonication (Fernández-García *et al.*, 2020b).

1.6.6. Reverse phase evaporation technique

In an organic solvent, phospholipid, hydrophobic drug, and edge activator are dissolved. By using a rotary evaporator, the entire organic solvent is extracted from the solution, leaving behind a dry film. The lipid film is redissolved in an organic solvent like isopropyl ether or diethyl ether rather than being hydrated. At this point, a two-phase emulsion is created when the aqueous phase is mixed into the organic phase. This system is then put through a sonication process to create a water-in-oil (w/o) emulsion. At the end, the organic solvent is once more evaporated to create a thick gel, which subsequently creates a suspension of vesicles (Alvi *et al.*, 2011).

1.6.7. Ethanol injection method

First, an organic solution is made by combining a lipid, surfactant, lipophilic substance, and an organic solvent (ethanol). Hydrophilic materials are dissolved in phosphate buffer solution to create the aqueous phase. Both solutions are heated for a specific period of time to a temperature between 40 and 50 °C. The aqueous solution is then continuously magnetically stirred as ethanolic solution is added dropwise. The finished formulation is sonicated to produce smaller-sized particles after the ethanol is evaporated using a rotary evaporator (Balata *et al.*, 2020).

1.7. Rationale of Study

The rationale of this research was to enhance the penetration of both drugs loaded in nanotransfersomes and to improve the macrophage internalization and anti-leishmanial potential.

1.8. Aim and Objectives

1.8.1. Aim

Aim of the study was to develop Nitazoxanide and Quercetin Co-loaded Nanotransfersomes (NTZ-QUR-NT) and incorporate them into chitosan gel to prepare Nitazoxanide and Quercetin Co-loaded Nanotransfersomal gel (NTZ-QUR-NTG) for the treatment of CL.

1.8.2. Objectives

- To optimize and characterize the NTZ-QUR-NT and NTZ-QUR-NTG.
- In-vitro and ex-vivo evaluation of NTZ-QUR-NT and NTZ-QUR-NTG as compared to conventional gels.
- To investigate the anti-leishmanial potential of NTZ-QUR-NT in comparison to NTZ-QUR dispersion

CHAPTER 2

MATERIALS AND METHODS

2. MATERIALS AND METHOD

2.1. Materials

2.1.1. Chemicals and reagents

Quercetin was purchased from Sigma Aldrich (Hamburg, Germany) and Nitazoxanide was obtained from Macklin Biochemical Co., Ltd (Shanghai, China). Chitosan, Tween® 80, Methanol and Chloroform were procured from Sigma Aldrich (Tokyo, Japan). Phospholipon 90G (PL90G) was gifted by lipoid AG, Switzerland. Roswell Park Memorial Institute (RPMI) medium-199 and penicillin/streptomycin were purchased from Thermo Fisher Scientific, USA. Potassium dihydrogen phosphate and Di-sodium hydrogen phosphate were acquired from Duksan Pure Chemicals, (Ansan-si, South Korea). Dialysis membranes of MWCO (12-14 kDa) were procured from Medicell Membranes Ltd, (London, UK). All other chemicals used in this study were of analytical grade.

2.1.2. Apparatus and equipment

Weighing balance (Ohaus corporation, PA 214C, USA), Rotary Evaporator (Heidolph Instruments GmbH & CO., Germany), pH meter (PH 700, EUTECH instruments, USA), Franz diffusion cell (PermeGear Inc., USA), UV-Visible Spectrophotometer (Halo DB-20, Dynamica, UK), Bath sonicator (Elmasonic GmbH, E60H, Germany), Centrifuge Machine (HERMLE Z 216 MK, Germany), Brookfield Rheometer (DV3T, MA, USA), Malvern Zetasizer (ZS-90, Worcestershire, UK), Magnetic Stirrer (Eisco Scientific, North America) Glass vials, volumetric flasks, eppendorf tubes, pipettes and stirrers, falcon tubes, petri dishes, and beakers (Sigma Aldrich, USA).

2.1.3. Animals and parasites

Male albino rats with age of 6-8 weeks and weights of 100-120 g were purchased from National Institute of Health (NIH), Islamabad. Animals were housed in standard facilities in accordance with the NIH recommendations for the care and management of laboratory animals. Moreover, ARRIVE guidelines were followed for animal study. Normal rat food and tap water was provided to the animals. Bioethical approval was obtained from bioethical committee of Quaid-i-Azam University, Islamabad, Pakistan (Protocol no BEC-FBS-QAU2021-364). *L. tropica* were procured from Khyber Medical University Peshawar KPK, Pakistan.

2.2. Methods

2.2.1. Preparation of NTZ-QUR co-loaded NT

NTZ-QUR co-loaded NT was prepared by using thin film hydration method. In the first step, Phospholipon 90G, edge activator (Tween® 80), nitazoxanide and quercetin was mixed in methanol and chloroform (1:1 v/v) to make organic phase. Then, in the next step to remove the organic solvents organic phase was transferred into rotary evaporator flask at 50 ºC and reduced pressure. Thin film was formed after evaporation of organic solvent and one hour hydration of this thin dried film was done with phosphate buffer saline at 60 ºC which was led to the formation of NTZ-QUR transferosomes as illustrated in **Figure 2.1**. Finally the formulation was sonicated for 5 min and after that the extrusion of NTZ-QUR-NT was done by 0.45 and 0.22 µm filter (Yuan *et al.*, 2022).

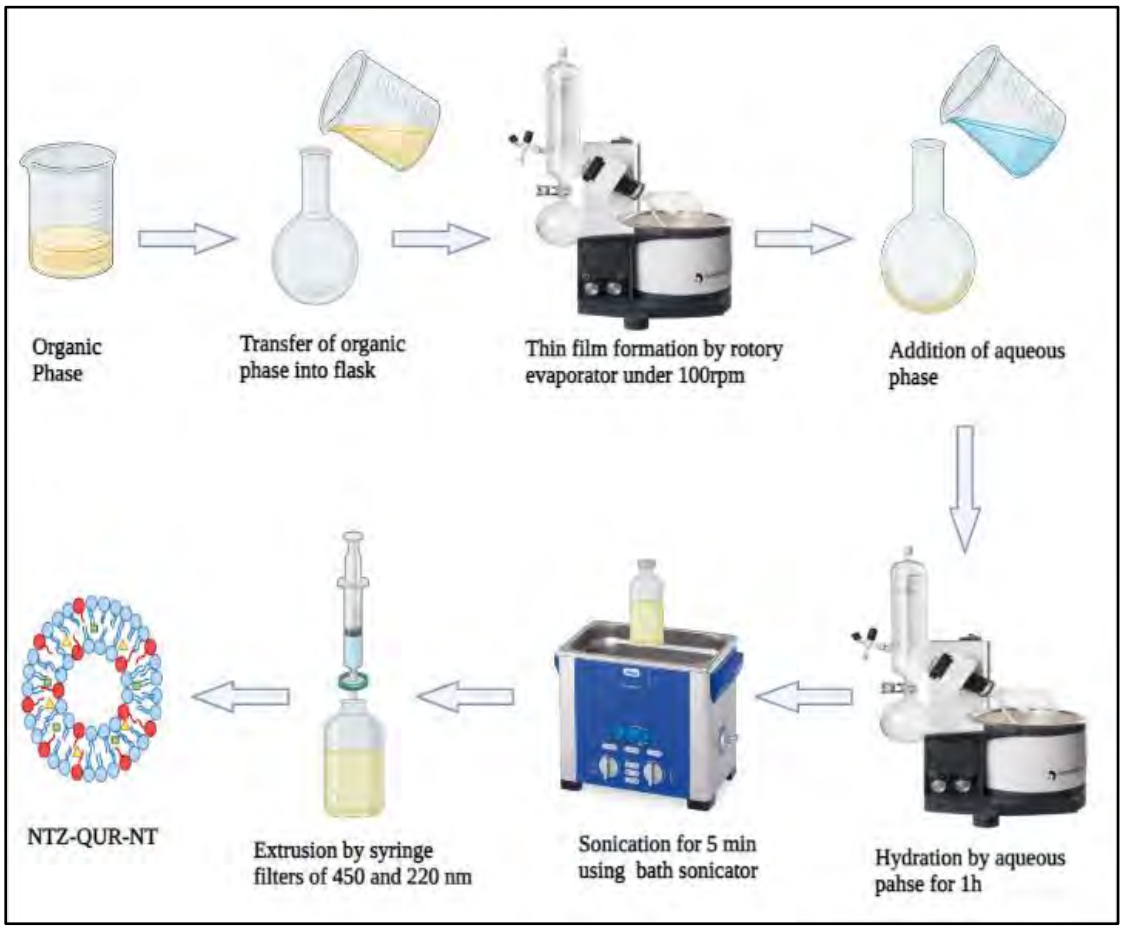

Figure 2.1. Preparation of NTZ-QUR-NT via thin film hydration. Figure is designed via Biorender

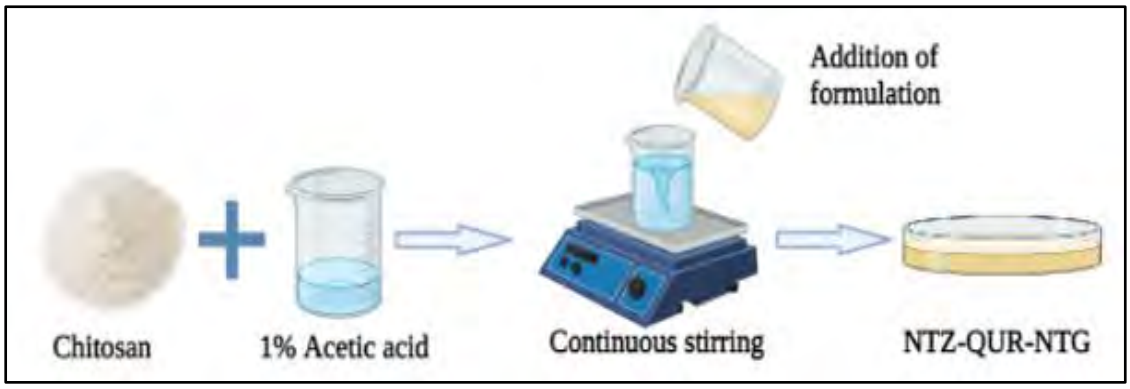

Figure 2.2. Preparation method of NTZ-QUR-NTG. Figure is designed via Biorender

2.2.2. Preparation of NTZ-QUR co-loaded NT gel (NTZ-QUR-NTG)

Chitosan powder was precisely measured at 100 mg and added to a solution of 1% acetic acid to create a volume of 2 ml while being continuously stirred. A final volume of 5 ml of NTZ-QUR-NTG was created by adding 3 ml of NTZ-QUR-NT with continuous stirring as illustrated in **Figure 2.2** (Salim *et al.*, 2020).

2.2.2.1. Acetic acid (1% v/v) solution preparation

One milliliter of acetic acid was mixed with one hundred milliliters of distilled water to create one percent acetic acid solution.

2.2.2.2. Chitosan gel preparation

Medium molecular weight chitosan was used to prepare the hydrogel. Blank hydrogel with 1%, 2% and 2.5% chitosan were developed in 1% acetic acid solution. At the end 2% chitosan gel was selected on basis of different physical parameters for NTZ-QUR-NTG preparation (Sohrabi *et al.*, 2016).

2.3. Characterization

2.3.1. Characterization of NTZ-QUR co-loaded NT

2.3.1.1. Particle size, PDI, ZP of NTZ-QUR-NT

These NTZ-QUR-NT parameters were examined utilizing dynamic light scattering at 25 °C using a Zetasizer ZS 90 equipped with a He-Ne laser operating at a wavelength of 635 nm. A static scattering angle of 90° was used for executing the measurements with software of 6.34 version (Malvern Instruments, Worcestershire, UK) for cumulative analysis. In order to dilute the samples before analysis, 10 µl of NTZ-QUR-NT were dissolved in 1 ml of de-ionized water (Din *et al.*, 2015; Rabia *et al.*, 2020).

2.3.1.2. Entrapment efficiency

The prepared NTZ-QUR-NT was subjected to centrifugation at 13,500 rpm for 3 hr using centrifuge (Hermle labortechnik, Z-206A, Germany). The pellet at the bottom of the eppendorf was removed from the free drug that was present in the supernatant. A UV spectrophotometer (Halo DB-20, Dynamica, UK) was used to observe the absorbances at 335 nm: λ_{max} of NTZ and 256 nm; λ_{max} of QUR, (Mahajan, 2018) to determine the concentrations of unentrapped drugs. This equation was used to determine percentage entrapment efficiency (%EE) of (Salim *et al.*, 2020).

$$\%\text{EE} = \frac{Total\ amount\ of\ drug - unentrapped}{Total\ amount\ of\ drug\ added} * 100$$

2.3.1.3. Transmission electron microscopy (TEM)

The NTZ-QUR-NT were subjected to a morphological analysis utilizing a TEM (Hitachi H- 7600; Tokyo, Japan) at a 100 kV accelerating voltage. To fix the particles on the carbon substrate, a tiny drop of sample was applied to the copper grid that had been coated with carbon. The sample was negatively stained with 2% phosphor tungstic acid after adhering to the carbon coating, followed by TEM examination (Khan *et al.*, 2021).

2.3.1.4. Fourier-transform infrared spectroscopy (FTIR)

FTIR (Nicolet-6700, Thermo Scientific, USA) was utilized to check any chemical interaction between QUR, NTZ, PL90G in NTZ-QUR-NT. Each sample was scanned at wavelengths from 400 to 4000 cm^{-1} followed by analysis observation using OMNIC™ software (version 7.3) (Khaleeq *et al.*, 2020).

2.3.1.5. Deformability index of NTZ-QUR-NT

The deformability index (DI) was measured using extrusion. For that purpose, a filter with a 100 nm pore size was used to process the samples. The Zetasizer was used to measure the size of the NTZ-QUR-NT formulation before and after extrusion (Rabia *et al.*, 2020).

$$DI = \frac{Size\ after\ extrusion}{Size\ before\ extrusion}$$

2.3.2. Characterization of NTZ-QUR-NTG

2.3.2.1. Organoleptic evaluation and pH measurement

Appearance, color, and homogeneity of blank and NTZ-QUR-NTG was examined physically and pH of the blank and NTZ-QUR loaded NT gel was evaluated by using digital pH meter (Psimadas *et al.*, 2012).

2.3.2.2. Rheology

Cone and plate Brookfield rheometer with a spindle CPA 42-Z (Brookfield Engineering Laboratories Inc., Middleborough, MA) was used for rheological evaluation of NTZ-QUR-NTG. A sufficient amount of gel was added to the receiving chamber, and runs were carried out there at temperature of 25 ºC with shear rates ranging from 1 to 100 s^{-1}. A rheogram was plotted between shear rate and viscosity of NTZ-QUR-NTG (Salim *et al.*, 2020).

2.3.2.3. Drug content

To determine the drug content of the NTZ-QUR-NTG, 5 mg of the was added into 5 ml of phosphate buffer saline (PBS) and kept for 24 hr. In next step, NTZ-QUR-NTG and PBS mixture was stirred for 30 min by using magnetic stirrer (Eisco Scientific, North America). Lastly, this solution was filtered and absorbance was observed with UV-visible spectrophotometer (Sujitha and Muzib, 2019).

2.3.2.4. Spreadability

Spreadability was determined by a reported method, briefly, a 2 cm area was marked on a glass slide and gel was placed on it. A second glass slide was placed over the gel and a 500 g weight will be placed on it for 5 min to allow the gel to spread (Ahad *et al.*, 2015). Afterward, the increase in the gel area was measured and the % spread area was calculated by using this formula:

$$\%Spread\ area = \frac{Final\ area\ after\ spreading}{2cm} * 100$$

2.3.3. Stability study

NTZ-QUR-NT and NTZ-QUR-NTG stability study was conducted at different temperatures including 4 and 25 ºC for a period of six months to evaluate the effects of storage conditions on stability of NTZ-QUR-NT and NTZ-QUR-NTG. For this purpose, samples were stored at respective storage condition. At certain time points (

0, 30, 90 and 180, days) NTZ-QUR-NT and NTZ-QUR-NTG were analyzed in terms of particle size PDI, ZP, color change, homogeneity and phase separation. (Jangdey *et al.*, 2017; Zahid *et al.*, 2022).

2.3.4. In-vitro drug release and kinetic study

The drug release from the NTZ-QUR-NT and NTZ-QUR-NTG was evaluated and compared with NTZ and QUR dispersion using a shaker water bath (Memmert SV 1422). To imitate the physiologically normal pH of blood and macrophages, a drug release study was carried out at pH 7.4 and 5.5, respectively. In a short, materials were weighed out and put into dialysis bags before being dialyzed in release media (phosphate buffer saline) of pH 7.4 and 5.5 in a shaker water bath. To maintain sink conditions, a fixed volume of samples was removed at regular intervals (0.25, 0.5, 1, 2, 4, 6, 8, 12 and 24 hr) and replaced with a comparable volume of fresh buffer. Evaluation of samples were done, and graph was plotted between %cumulative release of drug and time. Moreover, DD-solver was used to apply different kinetic models to determine the best fit model for drug release from NT and NTG (Rabia *et al.*, 2020).

2.3.5. Ex-vivo skin permeation and deposition study

Horizontal Franz diffusion cell apparatus was used to carry ex-vivo permeation experiment. The Franz diffusion cell, which has a 0.77 cm^2 permeation area and a 5.2 ml receiving compartment, was utilized. In order to keep the system's temperature at 32 °C, recently excised skin was put between the donor and receiving compartments. In a non-occlusive, open hydration system, test formulations were inserted in the donor compartment. Samples from the receiving compartment were taken at intervals of 0.5, 1, 2, 3, 4, 6, 8, 12 and 24 hr while replacing the sample with an equivalent volume of PBS. A graph showing the cumulative drug permeation per unit area vs time was created.

After the ex-vivo permeation investigation, the skin sections were dismounted, rinsed with distilled water to get rid of any leftover solution or formulation, and then blot dried. The SC was separated from the remaining skin layers using the tape stripping technique. With 15 to 20 layers of adhesive tape, the skin parts were stretched and peeled. By crushing the tape strips in methanol at 37 °C, the medicines were released from them, and the spectrophotometer was used to detect them. Following tape

removal, the remaining skin part was chopped into small pieces, crushed, and homogenized in methanol. The medicines were then quantified using a UV-visible spectrophotometer (Dar *et al.*, 2018).

2.3.6. Skin structure evaluation after treatment

Fourier-transform infrared spectroscopy (FTIR; Alpha Bruker ATR, Ettlingen, Germany) was used to assess the changes in epidermal lipid organization after applying NTZ-QUR-NTG and its comparison was done against normal skin. Because formulations created for transdermal application usually modify the structure of lipids, especially in the epidermis area. For this study, epidermis of rat skin was manually separated from the dermis by using isopropyl alcohol and distilled water at 60 °C. The epidermis was inserted between donor and receptor cells following complete skin layer separation, and NTZ-QUR-NT were applied for 4 hr under the same circumstances as for the penetration investigation. In order to analyze the functional group of skin membrane at wave number between 4000 to 650 cm^{-1}, the epidermal layer was removed after 4 hr, dipped in PBS to remove the formulation, dried, and then observed by FTIR (Rabia *et al.*, 2020).

2.3.7. Skin irritation study and histopathological study

The Draize scoring system was used in this study for skin evaluation. The rats were divided into three groups (positive, negative and treatment). Untreated rats were kept in negative control group and 0.8% formalin treated rats were considered as positive control group. Skins were observed for any sign of redness or edema and scoring was done at different time points (1, 24 ,48 ,72 hr). The results were further verified by histopathological examination. Cryostat microtome slices of skin samples were followed by microscopic inspection. (Batool et al., 2021).

2.3.8. Qualitative macrophage uptake study

Peritoneal macrophages (PMs) were used this uptake study. To extract the PMs, rat's peritoneal cavity was cautiously injected with 2 ml of 3% w/v sterile thioglycolate to avoid the bladder. After allowing the inflammatory response to last for four days, cervical dislocation was used to euthanize the rats. The peritoneal cavity was then filled with 5 ml of ice-cold RPMI 1640, and any peritoneal exudate was then collected. The exudate was centrifuged at 3000 rpm for 10 min, and the pellet was suspended in RPMI medium that had been supplemented with 10% fetal bovine serum (FBS), and 100 g/ml

streptomycin sulphate. In culture well plates, PMs had been incubated with rhodamine-labeled NTs (washed three times prior to the experiment) at a cell density of 2×10^4 cells. For comparisons plain rhodamine solution was as used as control. After 30 min in a CO_2 incubator, all samples were withdrawn to remove non-adherent cells by washing in phosphate buffer saline (PBS), and adhered cells were examined under a fluorescence microscope (Riaz *et al.*, 2019).

2.3.9. Quantitative macrophage uptake study

The NTZ-QUR-NTs and NTZ-QUR dispersion were planted in culture well plates in order to quantitatively measure the cellular absorption of NTs. After 24 hr, the plate was removed, and PBS cleaned. Scraping the adherent cells from slides allowed for their collection, which was then centrifuged. After that pellet were re-dispersed in methanol and sonicated for 5 min and then centrifuged one more time. Lastly, the concentration of NTZ and QUR was determined using an UV-visible spectrophotometer (Dar *et al.*, 2018).

2.3.10. Cell viability and toxicity assay

To determine the cytotoxicity of NTZ-QUR dispersion and NTZ-QUR-NT, previously isolated macrophages were put through a (4, 5-dimethylthiazol-2-yl)-2, 5-diphenyl tetrazolium bromide (MTT) experiment. The MTT assay uses mitochondrial succinate dehydrogenase to turn a yellow-colored tetrazolium component into blue, insoluble formazan crystals. Isolated macrophages were seeded into a 96-well plate for the MTT assay, which was then incubated for 24 hr at 37 ºC in a 5% CO_2 incubator. NTZ-QUR dispersion and NTZ-QUR-NT were introduced to the well in varying concentrations and left to incubate for 24 hours. The wells were then filled with 20 ml of MTT solution, which was then incubated for 4 hr to create formazan crystals, which were subsequently liquefied with 100 ml of DMSO**.** Then, absorbance was determined at a wavelength of 540 nm using a microplate reader (BioTek, USA) (Nazari-Vanani *et al.*, 2018). Percent cell viability was calculated by using following equation.

$$\%\, Cell\ viability\ = \frac{Absorbance\ of\ sample}{Absorbance\ of\ control} * 100$$

2.3.11. In-vitro anti-leishmanial activity analysis against *L. tropica*

An in vitro anti-leishmanial investigation was carried out by using MTT assay. At 24 °C, parasites were grown in RPMI medium that contained 10% fetal bovine serum (FBS), 100 IU/ml penicillin, and 100 g/ml streptomycin sulphates. Neubauer hemocytometer was used to count the promastigotes that were seeded at a density of 1×10^6 promastigotes/ml in each well of a 96-well plate containing 20 µl samples. DMSO and amphotericin B were regarded as negative and positive controls, respectively. The culture plates underwent a 72 hr incubation period at 24 °C. Each culture plate received a pre-filtered MTT solution with a concentration of 4 mg/ml that was formulated in distilled water. The plates were again incubated for 24 hr at 24 °C. After 4 hr, the plates' supernatant was carefully removed without disturbing the sediment that contained colorful formazan. Formazan crystal dissolution was accomplished by adding DMSO (100 µl) to the sediment. After one hr, the absorbance at a wavelength of 540 nm was measured using microplate reader. The IC_{50} were calculated by using GraphPad Prism® software (version 5) (Salim et al., 2020a).

2.3.12. Determination of combination index

Combination index (CI) was calculated to assess the cumulative therapeutic impact resulting from co-delivery of NTZ and QUR. The value of CI < 1 shows synergistic behavior while CI >1 shows antagonistic behavior. But if the value of CI is equal to 1 it shows additive effect (Emamzadeh *et al.*, 2018). CI was calculated by using this formula:

$$CI = \frac{IC_{50}(A+B)}{IC_{50}(A)} + \frac{IC_{50}(A+B)}{IC_{50}(B)}$$

where the IC_{50} values for each drug separately are denoted by IC_{50} (A) and IC_{50} (B). while IC_{50} (A + B) represents the IC_{50} of drugs combination.

2.4. Statistical analysis

Statistical analysis and optimization for formulation development were carried out using Design Expert® Software (version 12). However, GraphPad Prism® (version 5) and Microsoft Excel 365 (version 2010) were used to examine all other results. To get the p-values of tested formulations, they were checked in triplicate. One-way AVOVA and Student t-test were also used for statistical analysis. Statistics were significant for

measurements with a *p*-value less than 0.05. Additionally, the results were all reported as Mean ± Standard deviation.

CHAPTER 3

RESULTS

3. RESULTS

3.1. Standard Curve of NTZ and QUR

Standard curve of NTZ was made in acetonitrile at 335 nm and of QUR was made in methanol at 256 nm respectively. R^2 values of each standard curve was above 0.999, which indicates that they were best fitted.

Table 3.1. At different concentrations absorbances values of NTZ

Concentration of NTZ (µg/ml)	Absorbance
10	2.263
5	1.135
2.5	0.541
1.25	0.238
0.625	0.086
0.3125	0.026

Table 3.2. At different concentrations absorbances values of QUR

Concentration of QUR (µg/ml)	Absorbance
10	2.830
5	1.467
2.5	0.821
1.25	0.460
0.625	0.245
0.3125	0.138

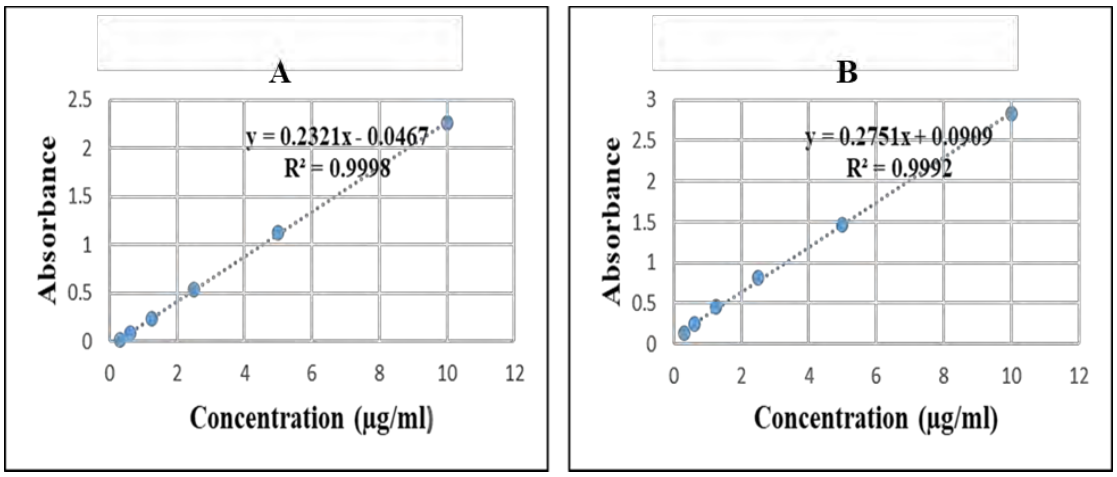

Figure 3.1. Standard curve of NTZ (A) and QUR (B)

3.2. Calibration curves of NTZ at pH 5.5 and 7.4

Calibration curve of NTZ was developed at pH 5.5 and 7.4 to determine the unknown concentrations of NTZ. The R^2 values in each graph was greater than 0.999, indicating the curves were best fitted.

Table 3.3. Absorbance values of NTZ at different concentrations at pH 5.5 and 7.4.

Sr.no	Concentration (µg/ml)	Absorbance at pH 5.5	Absorbance at pH 7.4
1	20	1.309	0.832
2	10	0.728	0.443
3	5	0.419	0.244
4	2.5	0.278	0.144
5	1.25	0.198	0.089

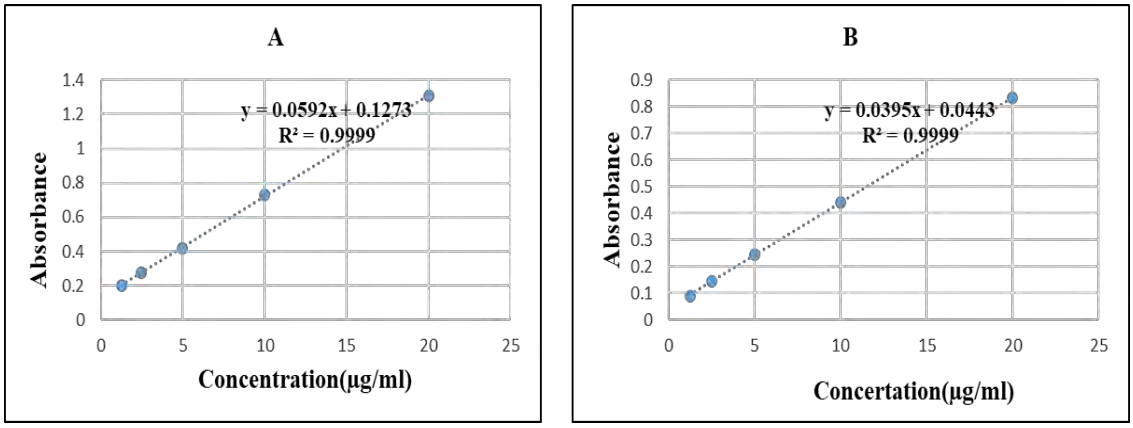

Figure 3.2. Calibration curve of NTZ at pH 5.5 (A) and 7.4 (B)

3.3. Calibration Curve of QUR at pH 5.5 and 7.4

Calibration curve of QUR was also developed at pH 5.5 and 7.4 to determine its unknown concentrations. The R^2 values in each graph was greater than 0.999, indicating the curves were best fitted.

Table 3.4. Absorbance values of QUR at different concentrations at pH 5.5 and 7.4.

Sr.no	Concentration (µg/ml)	Absorbance at pH 5.5	Absorbance at pH 7.4
1	20	1.893	1.167
2	10	1.043	0.615
3	5	0.596	0.316
4	2.5	0.381	0.185
5	1.25	0.259	0.098

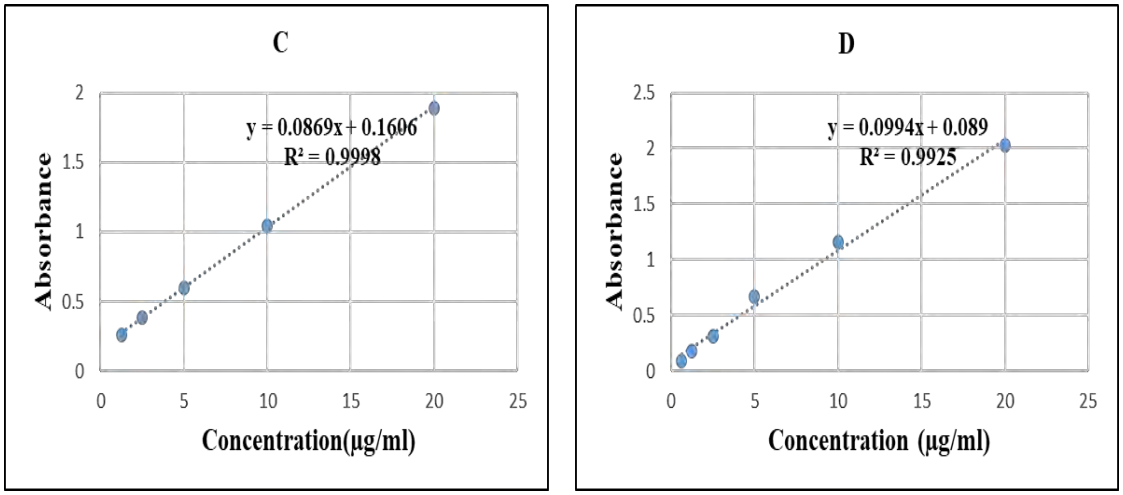

Figure 3.3. Calibration curve of QUR at pH 5.5 and 7.4 (D)

3.4. Optimization of NTZ-QUR-NT

For optimization of NTZ-QUR-NT Box-Behnken design (BBD) of software Design Expert® Ver .12 (State ease) was utilized. After employing certain maximum and minimum limits of independent variables the software suggested 13 formulations. All suggested formulations were prepared shown in **Figure 3.4**. The optimized formulation (NT3) has particle size of 210.9 ± 3.67 nm, PDI of 0.155 ± 0.009, ZP of -15.06 ± 1.48 mV as shown in **Figure 3.5 and 3.6** with little variation from predicted values of BBD. %EE of NTZ and QUR in optimized formulation was 88.04 ± 0.01% and 85.14 ± 0.02%, respectively.

Figure 3.4. Prepared formulations of NTZ-QUR-NT

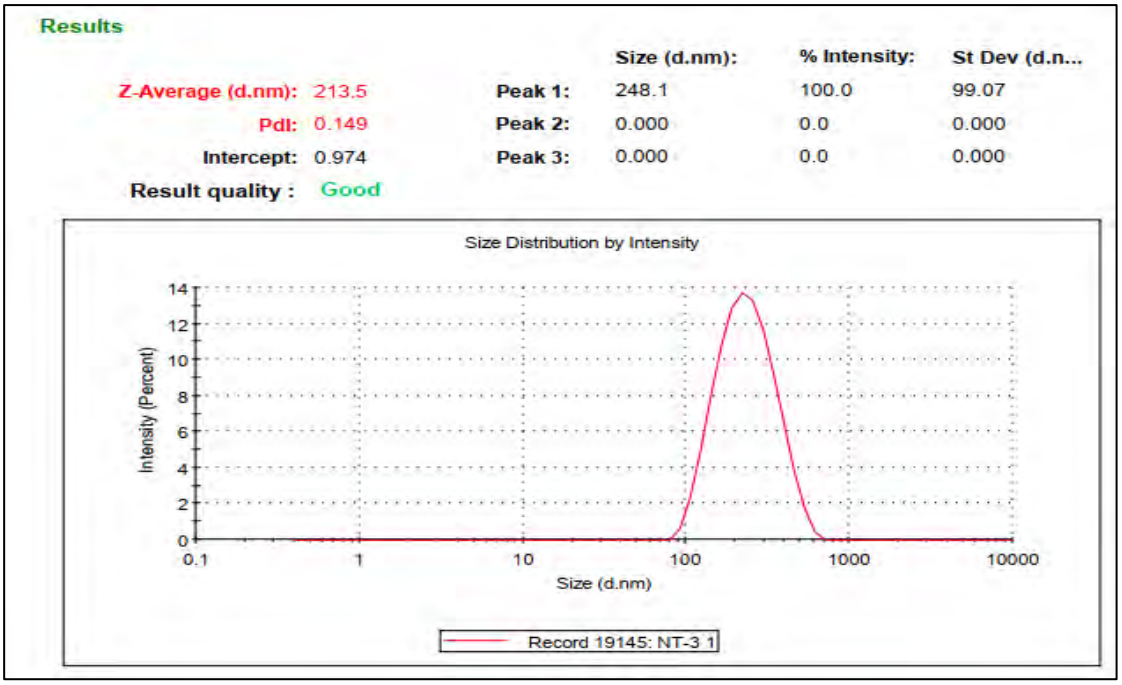

Figure 3.5. Particle size and PDI of optimized formulation

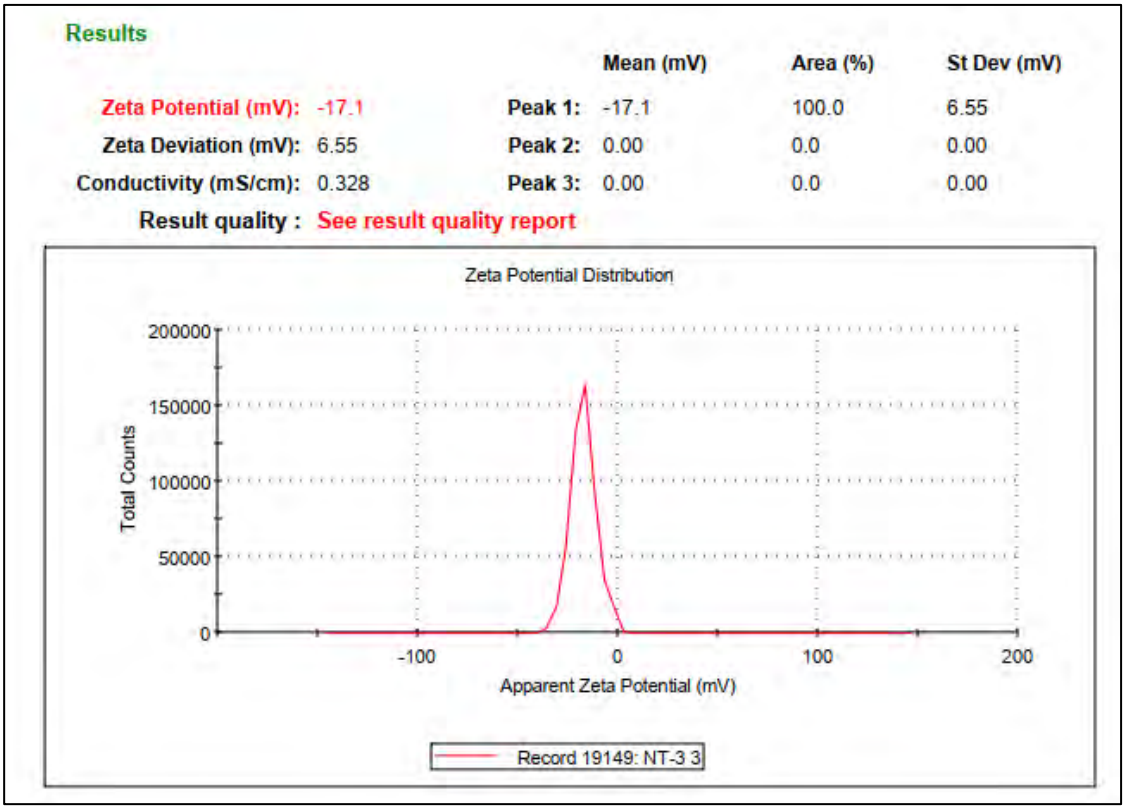

Figure 3.6. ZP of optimized formulation

Table 3.5. Optimization table of the NTZ-QUR-NT using Design Expert via Box-Behnke design.

Run	Lipid (mg)	Surfactant (mg)	QUR (mg)	NTZ (mg)	Particle Size (nm)	PDI	ZP (mV)	EE of QUR (%)	EE of NTZ (%)
NT-1	95	5	4	3	256.00 ± 0.70	0.288 ± 0.030	-18.6 ± 3.30	81.21 ± 0.11	89.92 ± 0.03
NT-2	87.5	12.5	4	3	205.12 ± 5.02	0.120 ± 0.007	-11.58 ± 0.52	76.14 ± 0.01	82.01 ± 0.01
NT-3	95	12.5	5	3	210.90 ± 3.67	0.155 ± 0.009	-15.06 ± 1.48	85.14 ± 0.02	88.04 ±0.01
NT-4	80	12.5	5	3	186.60 ± 1.12	0.095 ± 0.019	-8.25 ± 0.07	72.08 ± 0.04	79.03 ± 0.10
NT-5	80	12.5	3	3	177.01 ± 1.36	0.092 ± 0.019	-8.95 ± 0.07	68.03 ± 0.04	81.20 ± 0.10
NT-6	95	12.5	3	3	209.95 ± 1.19	0.144 ± 0.019	-12.10 ± 1.41	77.09 ± 0.15	89.01 ± 0.01
NT-7	87.5	20	5	3	195.60 ± 0.19	0.102 ± 0.007	-9.78 ± 0.07	78.70 ± 0.03	78.01 ± 0.06
NT-8	87.5	20	3	3	190.80 ± 5.83	0.104 ± 0.012	-9.06 ± 0.16	65.95 ± 0.01	80.01 ± 0.02
NT-9	80	5	4	3	222.60 ± 4.10	0.246 ± 0.054	-16.10 ± 2.12	74.67 ± 0.01	83.01± 0.19
NT-10	87.5	5	5	3	241.25 ± 0.91	0.236 ± 0.014	-20.09 ± 0.28	67.03 ± 0.11	86.65 ± 0.01
NT-11	80	20	4	3	156.25 ± 5.83	0.085 ± 0.064	-7.96 ± 1.17	69.64 ± 0.01	76.05 ± 0.01
NT-12	95	20	4	3	202.20 ± 0.70	0.154 ± 0.009	-8.01 ± 0.59	79.53 ± 0.18	85.01 ± 0.03
NT-13	87.5	5	3	3	229.60 ± 0.55	0.216 ± 0.007	-17.23 ± 2.86	74.70 ± 0.02	87.94 ± 0.01

Note: *QUR: Quercetin, NTZ: Nitazoxanide, PDI: Poly dispersity index, ZP: Zeta potential, EE: Entrapment Efficiency. Data is represented as Mean ± Standard deviation (n=3)*

3.4.1. Regression analysis of Box-Behnke design

Using Design Expert® software (version 12), the regression analysis of each, including PDI, ZP, particle size and entrapment efficiency was performed. The obtained results indicated that the models produced for each response were significant ($p < 0.05$) as shown in **Table 3.6**. The given model may navigate the design space based on the calculation of adequate precision for each answer because the value of adequate

precision greater than 4 are favorable.

Table 3.6. Regression analysis of Box-Behnken design for all responses.

Responses	R^2	Predicted R^2	Adjusted R^2	Adequate precision
Particle size (nm)	0.8952	0.8667	0.7762	18.2986
PDI	0.8587	0.8201	0.7010	15.5024
ZP (mV)	0.8469	0.8052	0.6815	13.3087
%EE of QUR	0.9198	0.8979	0.8286	20.1710
%EE of NTZ	0.9474	0.9330	0.9070	26.9197

3.4.2. Effect of independent factors on particle size

For dermal delivery in cutaneous leishmaniasis the particles size is considered as a key factor. For optimal macrophage uptake in dermal skin layer the particle should not be less than 100 nm and greater than 300 nm (Dar *et al.*, 2018). All the 13 formulations suggested by Design Expert® software were fabricated, having particle size fluctuating between 156.25 ± 5.83 nm and 256.50 ± 0.707 nm (shown in **Table 3.5**). Lipid and surfactant concentrations have significant effect on NTZ-QUR-NT particle size, with *p* values of 0.0002 and 0.0001, which is depicted graphically in **Figure 3.7**. On the other hand, QUR concentration has non-significant ($p = 0.2860$) effect on particle size of NTZ-QUR-NT. With increase in lipid concentration the particle size of NTZ-QUR-NT also increased, as reported in various other studies (Salim *et al.*, 2020; Batool *et al.*, 2021). Keeping surfactant and QUR constant particle size increased from 222.60 nm (NT-9) to 256.00 nm (NT-1) because of elevation in lipid concentration. However, the trend of surfactant concentration was contrary to the lipid concentration. Particle size of NTZ-QUR-NT were reduced with surge in surfactant concentration. As evident from NT-1 and NT-12, the NTZ-QUR-NT particle size decreased from 256.00 nm to 202.20 nm when surfactant concentration increased from 5 mg to 20 mg.

3.4.3. Effect of independent factors on PDI

PDI is a very important variable in nano systems because its value directly shows the homogeneity and uniformity of particles in the nano formulation. If the value of PDI is less than 0.5, the nano system is considered as uniform and stable (Salama and Aburahma, 2016). Linear model was found to be significant in case of PDI after applying ANOVA test. Herein, the lipid and surfactant were found controlling factors,

having *p* values 0.0008 and 0.0001, correspondingly. There was an inverse relation between surfactant concentration and PDI, as by increasing the concentration of surfactant there was significant decrease in PDI. As evident from results in **Table 3.5**, when surfactant concentration was increased from 5 mg to 20 mg, PDI was decreased from 0.246 (NT-9) to 0.085 (NT-11). On the contrary, increase in lipid content from 80 mg to 95 mg cause surge of PDI from 0.092 (NT-4) to 0.155 (NT-3). However, QUR concentration has not markedly affected the PDI of NTZ-QUR-NT.

3.4.4. Effect of independent factors on ZP of NTZ-QUR-NT

Stability of formulation mainly depends on the charge of nanoparticles. ZP values in range between -25 to +25 is considered as indicator of good stability (Shah *et al.*, 2014). Both lipid and surfactant have significant effect (*p* value 0.0345, 0.001) on ZP of formulation. The negative charge on formulation is attributed to the Phospholipon 90G which form double layer of nano vesicles (Batool *et al.*, 2021). As noticeable from the **Table 3.5** when concentration of lipid was increased from 80 mg to 95 mg, there was escalation in the negative charge on particles from -8.25 mV (NT-4) to -15.06 mV (NT-3). In contrast, when the concentration of surfactant (Tween® 80) was increased from 5 mg to 20 mg, there was significant decrease in negative charge on the particles from -20.09 mV (NT-10) to -9.78 mV (NT-7).

3.4.5. Effect of independent factors on %EE of NTZ and QUR.

The effectiveness of nanoparticles mainly depends on entrapment of drug, thus it is considered a very important parameter for optimization of nanoparticles (Alam *et al.*, 2012). All the independent factors: lipid, surfactant and QUR have significant effect on the entrapment of NTZ and QUR as depicted in **Figure 3.10** and **3.11**. As the concentration of lipid increased from 80 mg to 95 mg %EE of NTZ enhanced from 76.05% (NT-11) to 85.01% (NT-12) and for QUR from 69.64% to 79.53%. On the contrary, when content of surfactant increased from 5 mg to 20 mg %EE of NTZ decline from 83.01% (NT-9) to 76.05% (NT-11) and QUR from 74.67% to 69.64%. Lastly, 4% increase in %EE of QUR was observed with surge in the concentration of QUR from 3 mg to 5 mg.

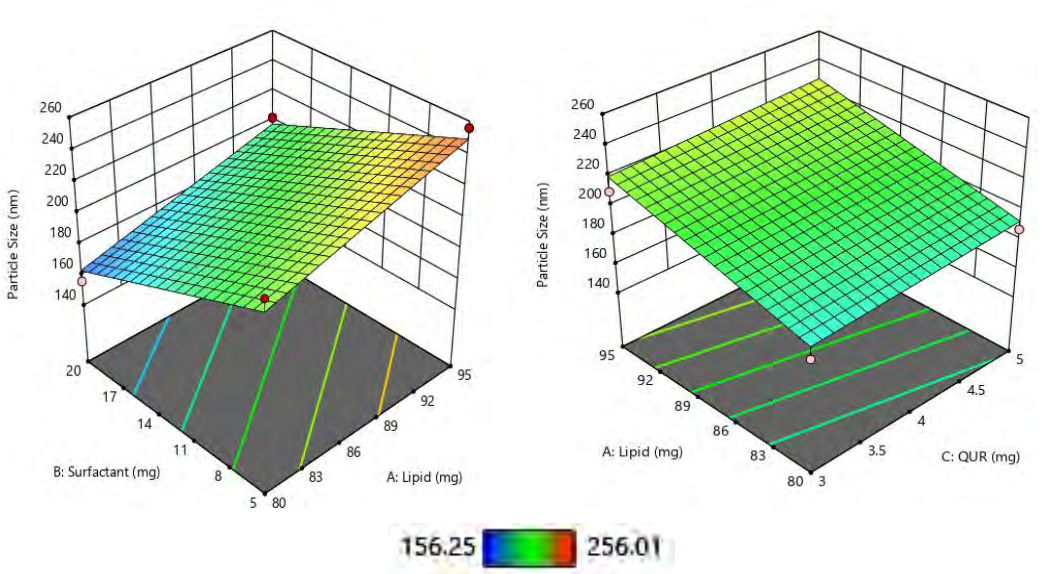

Figure 3.7. 3D response surface graph showing effect of lipid, surfactant and QUR on particle size

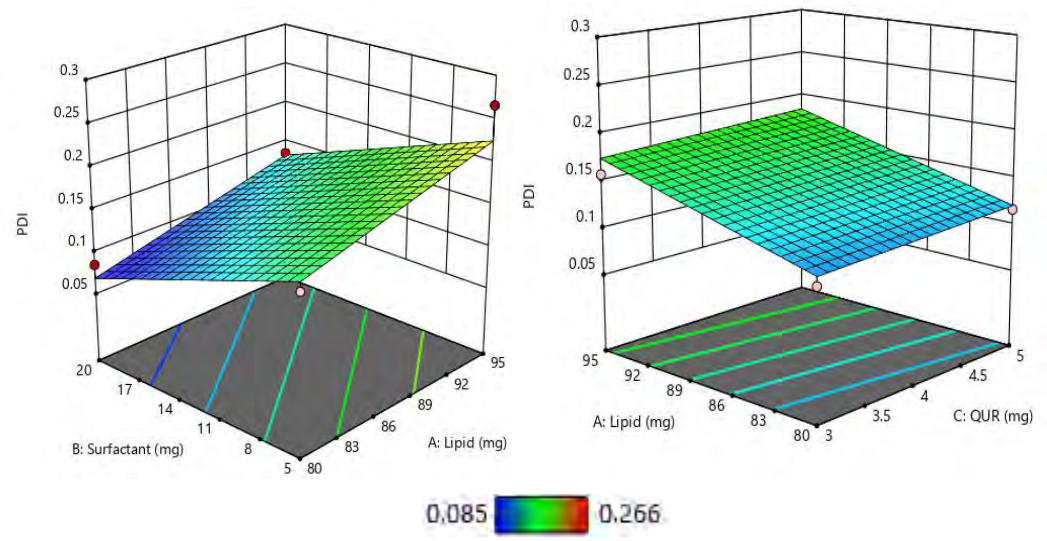

Figure 3.8. 3D response surface graph showing effect of lipid, surfactant and QUR on PDI

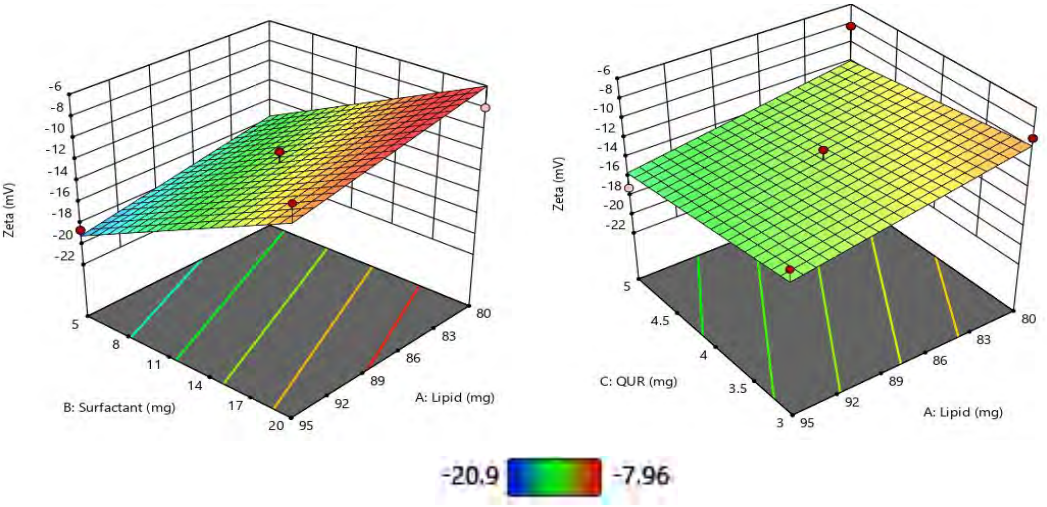

Figure 3.9. 3D response surface graph showing effect of lipid, surfactant and QUR on ZP

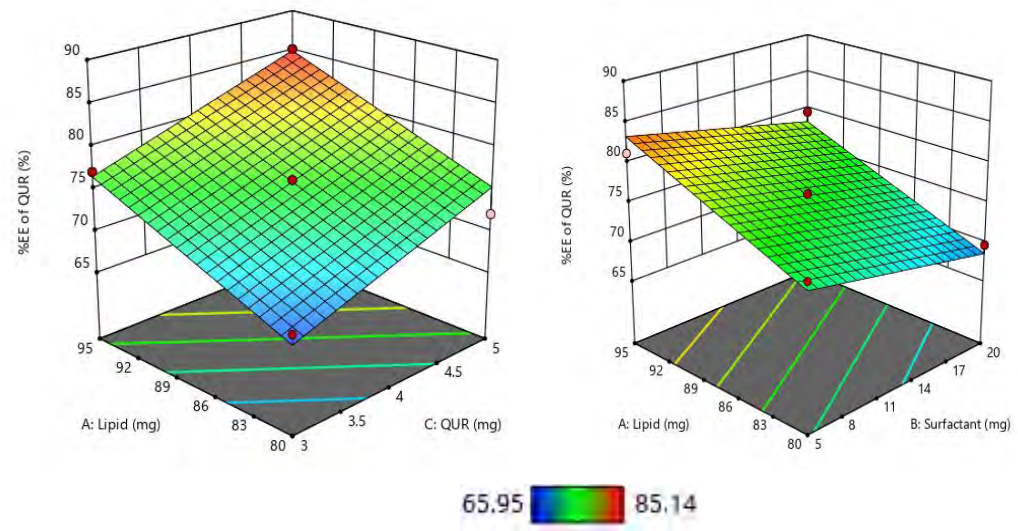

Figure 3.10. 3D response surface graph showing effect of lipid, surfactant and QUR on % EE of QUR

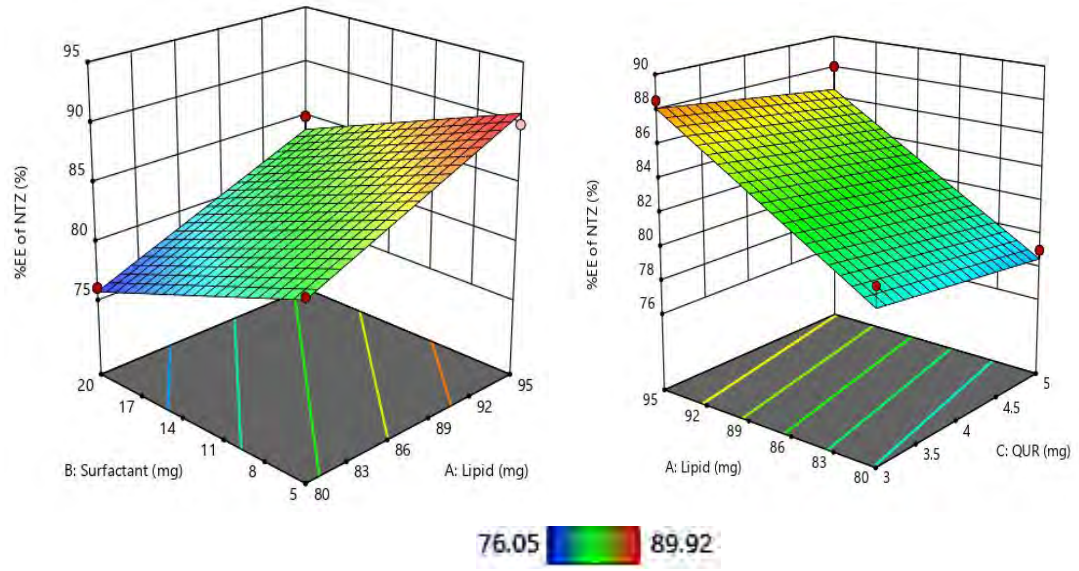

Figure 3.11. 3D response surface graph showing effect of lipid, surfactant and QUR on % EE of NTZ

3.5. TEM Analysis of NTZ-QUR-NT

TEM analysis of NTZ-QUR-NT was performed. The TEM image showed that NT had uni-lamellar and spherical shape. The particles size was less than 250 nm with uniform distribution as shown in **Figure 3.12**.

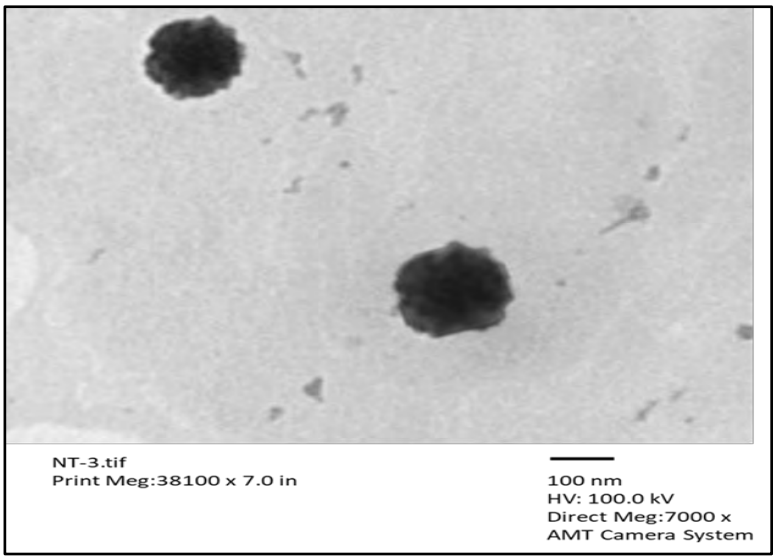

Figure 3.12. TEM image of the optimized formulation (NT-3)

3.6. Deformability Index (DI) of NTZ-QUR-NT

Deformability is a unique feature of transfersomes which makes it possible for them to pass through the tight junctions of skin with ease, especially from upper skin layers when used as a carrier for topical delivery. With the presence of edge activator (Tween® 80), transfersomal vesicles acquire this deformability property. The edge activator, thus plays a significant role, in the targeted delivery of drugs via NT. DI value of the NTZ-QUR-NT was used to evaluate its stress-dependent flexibility and shape change (Kang *et al.*, 2010; Batool *et al.*, 2021). A value closer to 1 indicates that the vesicles are more deformable. The deformability index has a range of 0 to 1 (El Zaafarany *et al.*, 2010). NTZ-QUR-NT deformability index was discovered to be 0.9264 ± 0.042. It is reported that the increase in content of Tween® 80, makes vesicles more deformable. This may be due to its long carbon chain, which is non bulky and highly pliable which provide flexibility to lipid bilayer (Zeb *et al.*, 2016).

3.7. FTIR Analysis to Assess the Compatibility of Excipients with Drugs

FTIR analysis of NTZ, QUR, PL90G, physical mixture (PM) and NTZ-QUR-NT performed to check chemical interaction among the constituents of the formulation. FTIR spectrum of NTZ, QUR and PL90G showed characteristic peaks as presented in **Figure 3.13**. Stretching at 3358.91 cm^{-1},1774.94 cm^{-1} and 1524.92 cm^{-1} correspondingly represents N-H, C=O and N=O functional groups of NTZ. Vibrations at 3402.15 cm^{-1} and 3213.71 cm^{-1} showed the presence of hydroxyl groups (OH) of QUR. Peaks at 1610.91 cm^{-1} and 1010.21 cm^{-1} represents C=C stretching of alkyne

group and C-C bending of alkyl group of QUR. Characteristic band at 2924.09 cm^{-1} and 2855.03 cm^{-1} exhibits hydrocarbons stretching of PL90G. FTIR spectra of PM and NTZ-QUR-NT indicated all the specific peaks of NTZ, QUR and PL90G which clearly showed the compatibility of drugs and excipients in formulation.

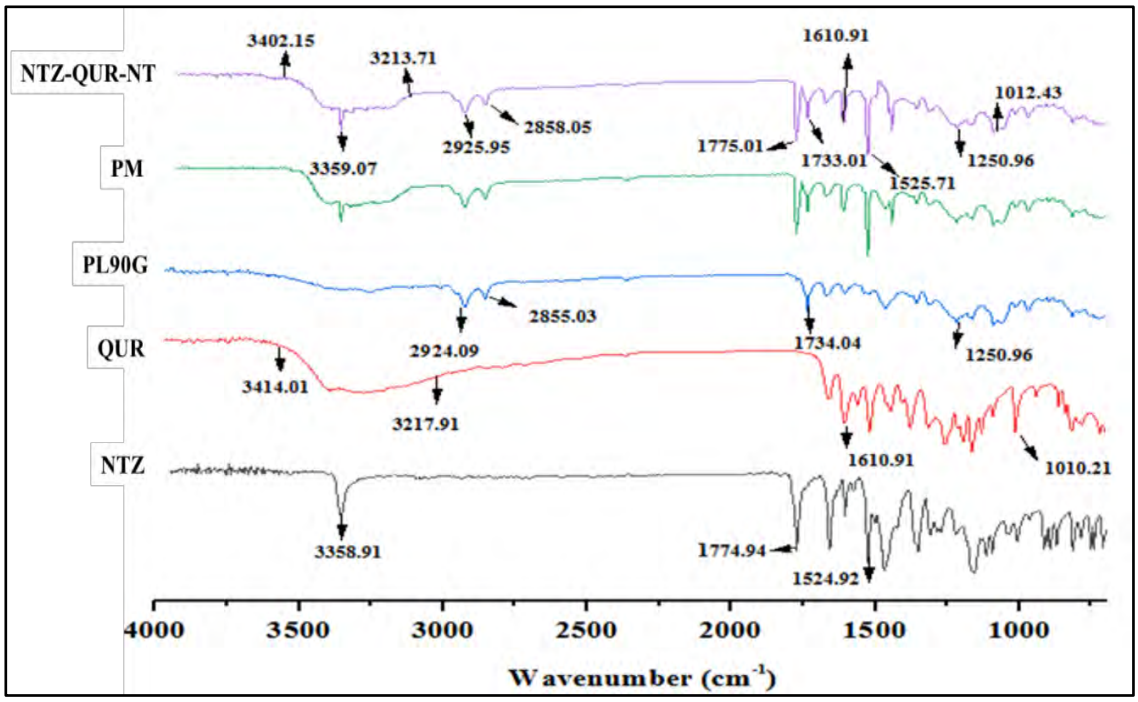

Figure 3.13. FTIR analysis of NTZ, QUR, PL90G, PM and NTZ-QUR-NT observed in range of 4000-400 cm^{-1}

3.8. NTZ-QUR-NTG physicochemical characterization

Physicochemical characterization of NTZ-QUR-NTG was carried out and it was observed that NTZ-QUR-NTG appearance was opaque yellowish in color with uniform homogeneity as shown in **Figure 3.14**. The pH of NTZ-QUR-NTG was 5.8 ± 1.56 and spreadability was 310.50 ± 3.5%, compatible for topical use (Ahad *et al.*, 2015). The drug content of NTZ and QUR was found to be 98.45 ± 1.17% and 97.86 ± 1.39%. Additionally, the impact of shear rate upon viscosity was examined using a Brookfield viscometer, and the results showed that, the viscosity of gel decrease with increase in shear rate. **Figure 3.15** depicts the shear thinning and pseudoplastic behavior of the gel.

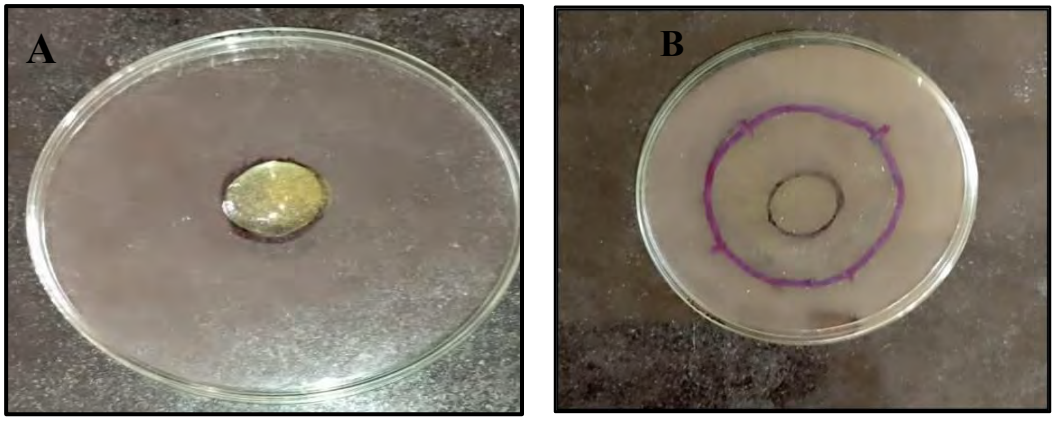

Figure 3.14. Physical appearance of NTZ-QUR-NTG (A), Spreadability of NT-QUR-NTG (B)

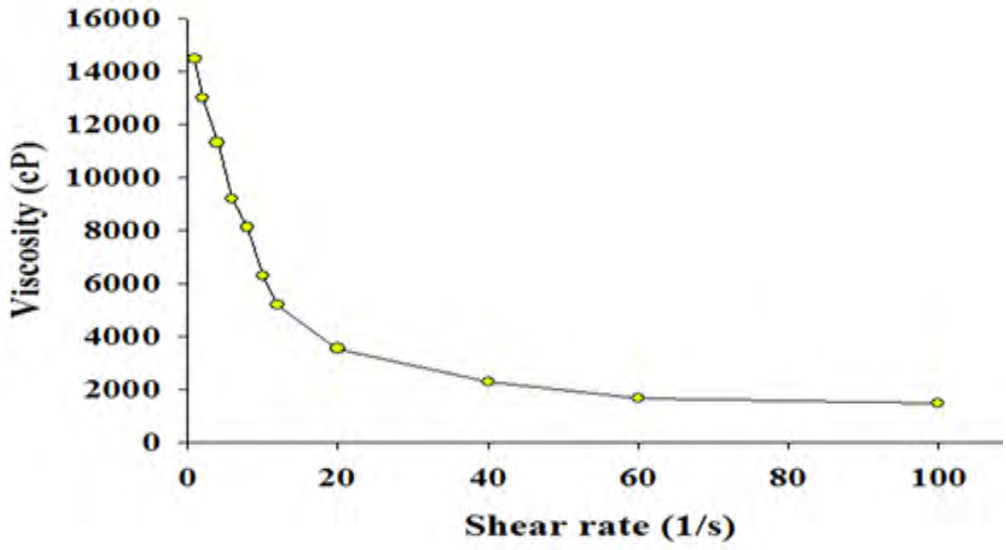

Figure 3.15. Graphical presentation of the effect of shear rate on viscosity of NTZ-QUR-NTG

Table 3.7. Characterization of the NTZ-QUR-NTG.

Physical Appearance	Yellowish opaque
Homogeneity	Uniform
Flow Behavior	Non-Newtonian flow
Drug content of NTZ	98.45 ± 1.17
Drug content of QUR	97.86 ± 1.39
pH	5.8 ± 1.56
Spreadability	310.50 ± 3.5%

3.9. Stability Studies

The stability study of NTZ-QUR-NT and NTZ-QUR-NTG was carried out for a period of six months at 4 and 25 °C, as shown in **Table 3.8 and 3.9**. NTZ-QUR-NT were assessed for particle size, PDI and zeta potential. Stability data showed that there was non-significant ($p > 0.05$) increase in NTZ-QUR-NT particle size from 213.50 ± 3.67 nm to 219.26 ± 4.14 nm (at 4 °C) and 222.62 ± 5.61 (at 25 °C), respectively. Similarly, there was negligible variation in PDI and ZP during storing conditions. The initial PDI and ZP values of optimized formulation were 0.155 ± 0.009 and -17.10 ± 1.48 mV. After duration of six month, it was found to be 0.218 ± 0.052 and -15.39 ± 0.07 correspondingly. NTZ-QUR-NTG was also analyzed in terms of precipitation, drug content and physical appearance. The stability study findings showed that there was no meaningful change in drug content of NTZ and QUR in NTZ-QUR-NTG. No change in color or precipitation was observed in NTZ-QUR-NTG during period of six month.

Table 3.8. Stability data of NTZ-QUR-NT.

Time period	At temperature 4 ± 2 °C			At temperature 25 ± 2 °C		
	Particle size (nm)	PDI	ZP (mV)	Particle size (nm)	PDI	ZP (mV)
0	213.50 ± 3.67	0.155 ± 0.009	-17.10 ± 1.48	213.50 ± 3.67	0.155 ± 0.009	-17.10 ± 1.48
1 month	215.71 ± 2.25	0.164 ± 0.009	-16.89 ± 1.56	217.21 ± 4.33	0.172 ± 0.041	-15.81 ± 1.22
3 months	217.04 ± 2.64	0.167 ± 0.007	-16.07 ± 1.52	219.17 ± 5.09	0.184 ± 0.095	-15.92 ± 1.59
6 months	217.26 ± 4.14	0.202 ± 0.012	-15.80 ± 1.37	222.62 ± 5.61	0.218 ± 0.052	-15.39 ± 0.07

Table 3.9. Stability data of NTZ-QUR-NT.

Time (month)	At temperature 4 ± 2 °C				At temperature 25 ± 2 °C			
	PDC of NTZ	PDC of QUR	Physical appearance	Precipitation	PDC of NTZ	PDC of QUR	Physical appearance	Precipitation

0	98.45 ± 1.17	97.86 ± 1.39	Uniform, no color change	No	98.45 ± 1.17	97.86 ± 1.39	Uniform, no color change	No
1	98.32 ± 1.07	97.72 ± 1.16	Uniform, no color change	No	98.29 ± 1.09	97.65 ± 1.12	Uniform, no color change	No
3	98.11 ± 1.98	97.51 ± 1.38	Uniform, no color change	No	98.22 ± 1.18	97.44 ± 1.88	Uniform, no color change	No
6	98.10 ± 1.09	97.40 ± 1.26	Uniform, no color change	No	97.84 ± 1.39	97.10 ± 1.21	Uniform, no color change	No

3.10. In-vitro Release Study of NTZ and QUR at pH 5.5

Release study was performed on physiological pH of skin macrophages endosomes (pH 5.5) and in-vitro release pattern of both drugs NTZ and QUR shown in **Figure 3.16 (A)** and **(B)**. At 4 hr, in simulated endosomal pH (5.5), 85% of the NTZ was released from NTZ dispersion, followed by a total (100%) drug release at 12 hr. Similarly, from NTZ-QUR-NT 62% of drug in first 4 hr followed by a total of 80% drug release at 24 hr. Unlike both of the above formulation, the NTZ-QUR-NTG significantly retarded the drug release, as only 27% of drug was released in first 4 hr, followed by 56% drug release in 24 hr. While in case of QUR, 100% of drug was released from QUR Dispersion within 6 hr. On the other hand, at 6 hr, 67% and 38% of drug was released from NTZ QUR NT and NTZ QUR NTG, respectively which followed by 85% and 60% of drug release in 24 hr.

3.11. In-vitro Release Study of NTZ and QUR at pH 7.4

In vitro release study of QUR and NTZ was also performed at physiological pH of blood (pH 7.4) as presented in **Figure 3.16 (C)** and **(D)**. 80% of NTZ was released from NTZ dispersion at first 4 hr. Unlike NTZ dispersion, 52% and 30% of drug was released from NTZ-QUR-NT and NTZ-QUR-NTG, respectively within 4 hr followed by 78% and 49% release after 24 hr. Release pattern of QUR from its dispersion was different from NTZ dispersion due to acidic nature of QUR. This nature accounts for the 100% release of drug in just 3 hr. In case of NTZ-QUR-NT and NTZ-QUR-NTG 40% and 25% drug was released in 3 hr, respectively and followed by drug release 76% and 42% in 24 hr.

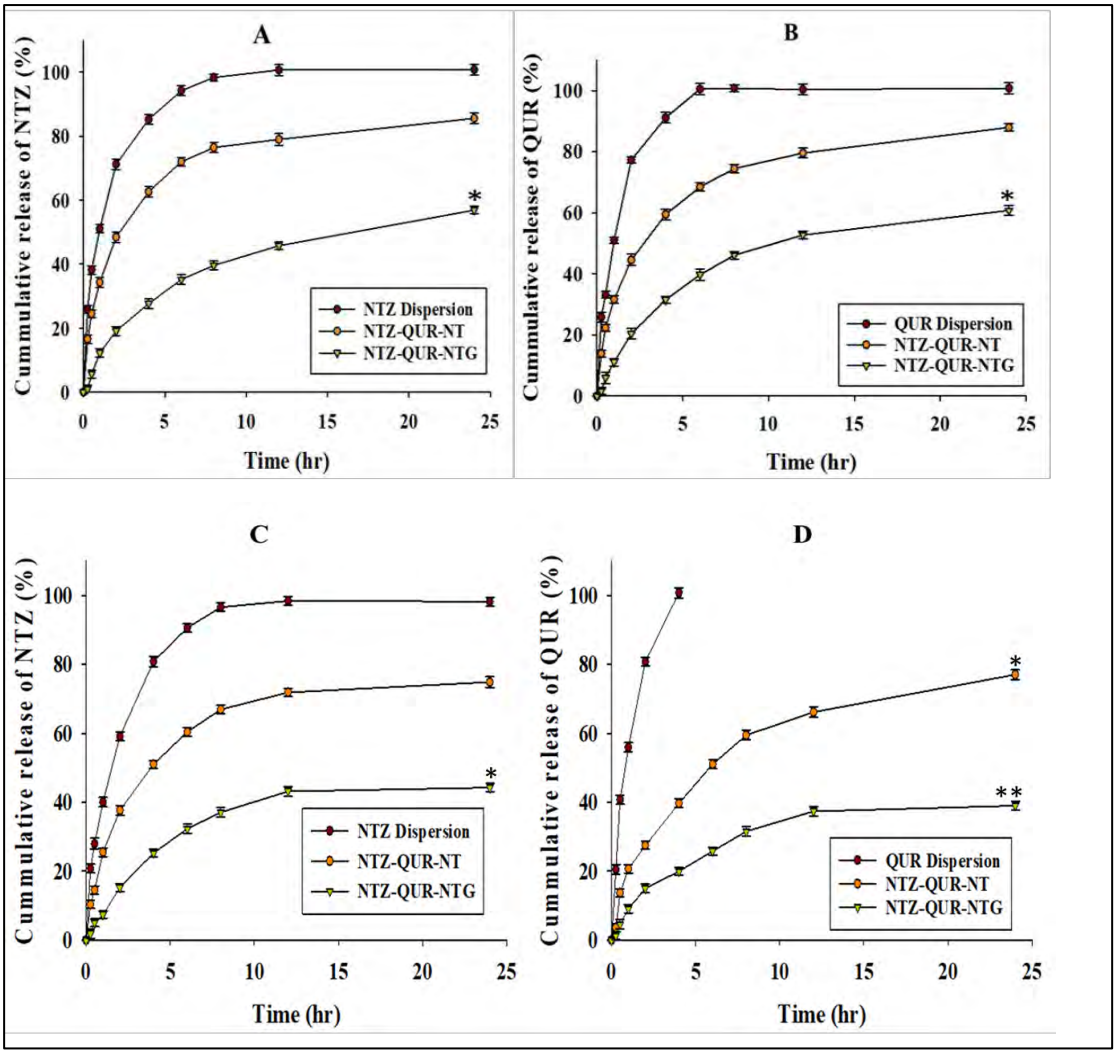

Figure 3.16. In-vitro release of NTZ at pH 5.5 **(A)**, In-vitro release of QUR at pH 5.5 **(B)**, In-vitro release of NTZ at pH 7.4 **(C)**, In-vitro release of QUR at pH 7.4 **(D)**. ***Note:*** *Data are represented as Mean ± Standard deviation (n=3), ** $p < 0.01$, * $p < 0.05$ as compared to NTZ and QUR Dispersion.*

3.12. Release Kinetic Study

To analyze the release pattern of QUR and NTZ from transferosomes and transferosomal gel different kinetic models (First order, zero order, Korsmeyer-Peppas, Hixon-Crowell, first order, Higuchi) were applied by utilizing DD-solver. In Table **3.10** R^2 value of all models are stated. By analyzing R^2 values of all models Korsmeyer-Peppas was considered as most fitting for release of both drugs from NT and Higuchi for NTG. Their kinetic model graphs are shown in figure. The value of n is the key factor of this model which was used to confirm that if the release of drugs from drug delivery system was via fickian or non-fickian diffusion. As the values of n were less than 0.45 in cases NTZ-QUR-NT and greater than 0.45 in case of NTZ-QUR-NTG which suggested that the release of QUR and NTZ was through fickian diffusion from

NT and non-fickian from NTG.

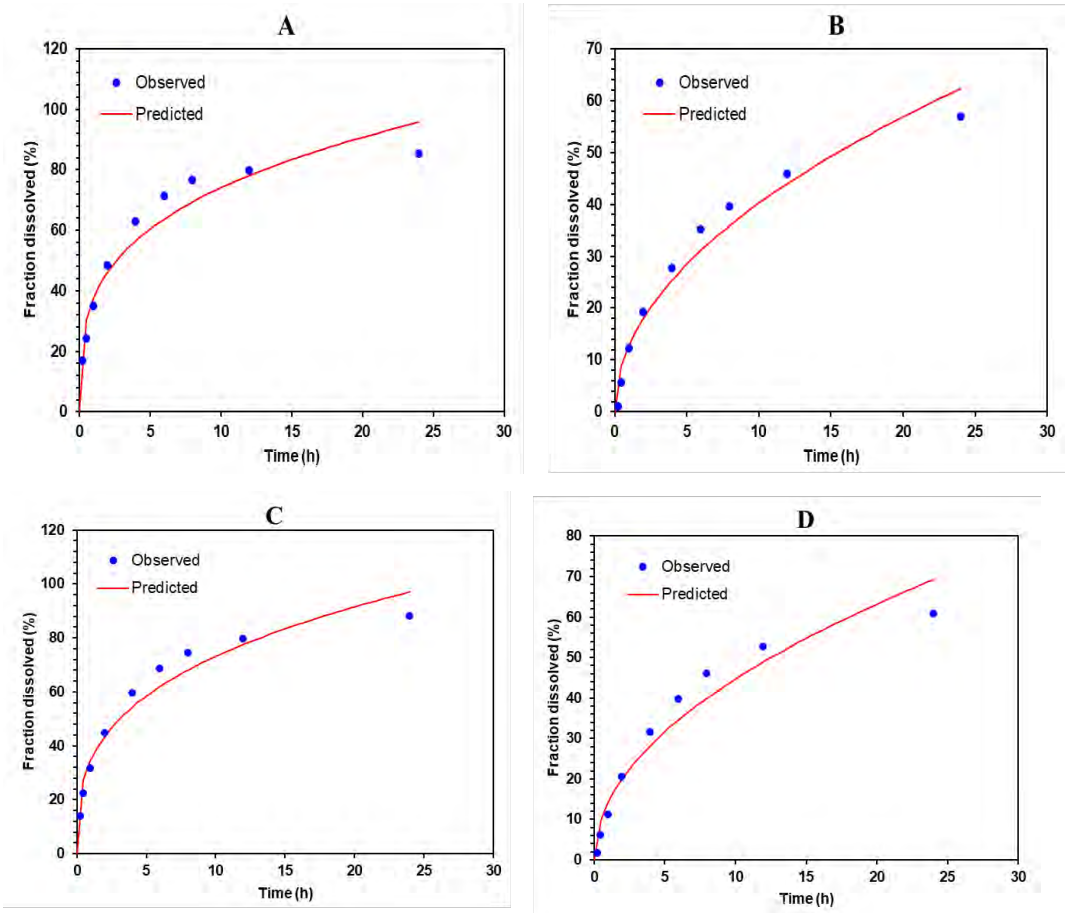

Figure 3.17. Observed and predicted values of Korsmeyer and Peppas model for NTZ release from NTZ-QUR-NT at pH 5.5 **(A)**, Higuchi model for NTZ release from NTZ-QUR-NTG at pH 5.5 **(B)**, Observed and predicted values of Korsmeyer and Peppas model for QUR release from NTZ-QUR-NT at pH 5.5 **(C)**, Higuchi model for QUR release from NTZ-QUR-NTG at pH 5.5 **(D)**

Table 3.10. R^2 values of all kinetic models.

Release Model	**R^2 Values of Release Model**			
	Nitazoxanide		**Quercetin**	
	NTZ-QUR-NT	**NTZ-QUR-NTG**	**NTZ-QUR-NT**	**NTZ-QUR-NTG**
Zero order	-0.8236	0.5248	-0.4158	0.4807
First order	0.7890	0.8160	0.8519	0.8374
Higuchi	0.6412	0.9724	0.7728	0.9511
Hixon-Crowell	0.6722	0.7398	0.7538	0.7516
Korsmeyer-Peppas(n)	0.9154 (0.292)	0.9596 (0.472)	0.9387 (0.323)	0.9369 (0.464)

3.13. Ex-vivo Skin Permeation and Deposition Studies

The cumulative amount of NTZ and QUR permeated from per unit area of rat skin from NTZ-QUR co-loaded NT was 248.23 µg/cm^2 and 316.26 µg/cm^2. While permeation of both drugs from NTZ-QUR co-loaded NT gel was 202.85 µg/cm^2 and 262.72 µg/cm^2 which was little less than NT due to controlling nature of chitosan gel. However, the permeation of NTZ and QUR from plain gels was only 40.541 µg/cm^2 and 59.37 µg/cm^2. by comparing the results and finding the enhancement ratios it was observed that the permeation of NTZ and QUR from our optimized formulation were increased 5-folds and 4 -folds as compared to plain gel.

The increased permeation of drugs from our nano formulation was due to the ultra-deformable nature of transferosomes which enabled them to pass through from five to ten times small pores of skin barrier (Cevc and Scha, 2002; Apsara *et al.*, 2020). Moreover, 38.74% and 34.97% of NTZ and QUR were deposited in deeper layers of skin (epidermis and dermis) from transferosomal gel whereas only 2.65% and 2.37% of both drugs were deposited from plain NTZ and QUR gel. Basically, the flexibility and trans epidermal hydration gradient of NT make them squeeze across SC but transcutaneous hydration gradient enabled them to remain entrapped in dermis which is desired in case of cutaneous leishmaniasis treatment (Dubey *et al.*, 2007; Avadhani *et al.*, 2017).

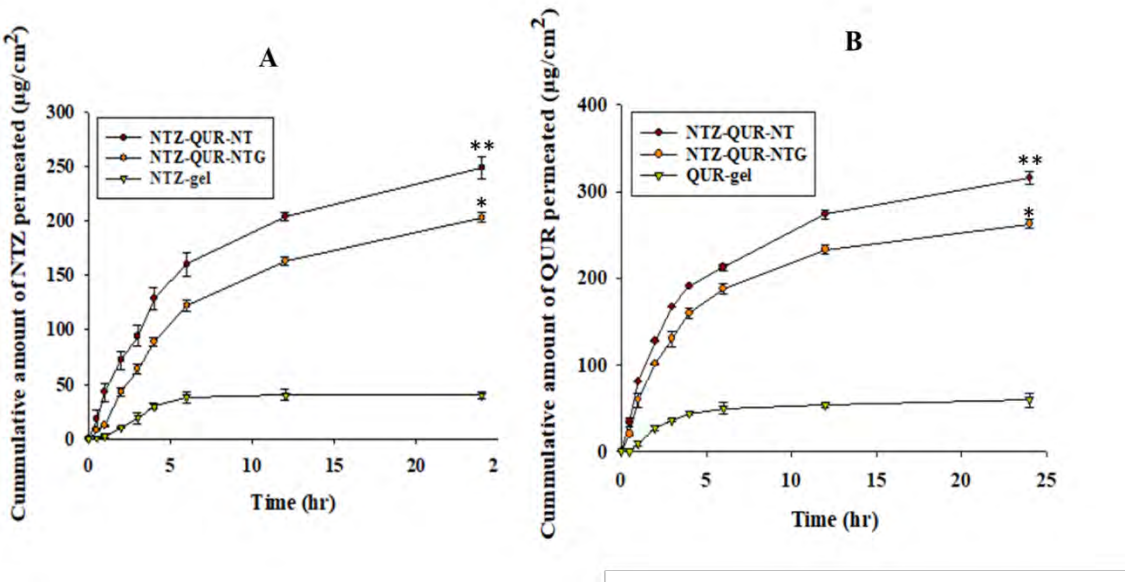

Figure 3.18. Ex-vivo permeation of NTZ (A), Ex-vivo permeation of QUR (B), Data are represented as

Mean ± Standard deviation (n=3), ** $p < 0.01$, * $p < 0.05$ as compared to NTZ and QUR gel.

Table 3.11. Skin permeation parameters of NTZ and QUR.

Formulation	Nitazoxanide		
	Total amount of drug permeated in 24 hr (µg/cm^2)	**Flux J_{max} (µg/cm^2/h)**	**Enhancement ratio**
NTZ-gel	40.541	1.689	1
NTZ-QUR-NT	248.23	10.34	6.12
NTZ-QUR-NTG	202.85	8.45	5.02
	Quercetin		
QUR-gel	59.37	2.47	1
NTZ-QUR-NT	316.26	13.19	5.34
NTZ-QUR-NTG	262.72	10.94	4.42

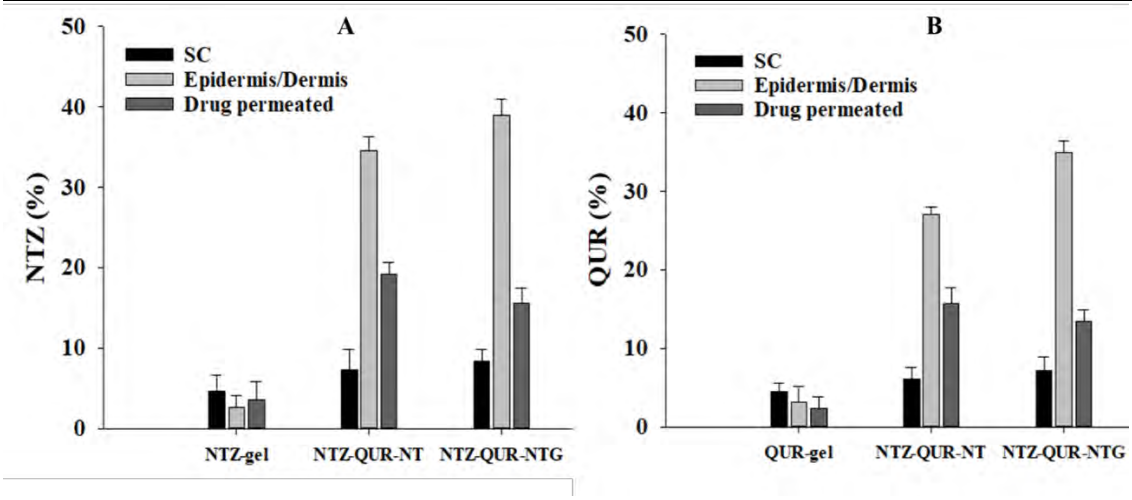

Figure 3.19. Skin deposition of NTZ (A) and QUR (B)

3.14. Skin Structure Evaluation After Treatment

After treatment with NTZ-QUR-NTG, the skin's FTIR was run to look for structural alterations and compared with normal skin as represented in **Figure 3.20**. On untreated and NTZ-QUR-NTG treated rat skin, FTIR analysis was done. The characteristic peak of C-H bond stretching at 2925.74 cm^{-1}and 2931.12 cm^{-1}, presented in FTIR spectrum of normal skin and NTZ-QUR-NTG treated skin, respectively. It showed that the integrity of the skin's hydrocarbon lipid bilayers was preserved after application of NTZ-QUR-NTG. For normal skin, amide group peaks were seen at 1633.19 cm^{-1} and 1544.09 cm^{-1}, while for skin treated with NTZ-QUR-NTG, peaks were seen at 1647.11 cm^{-1} and 1541.34 cm^{-1}, indicating no significant change in skin structure**.**

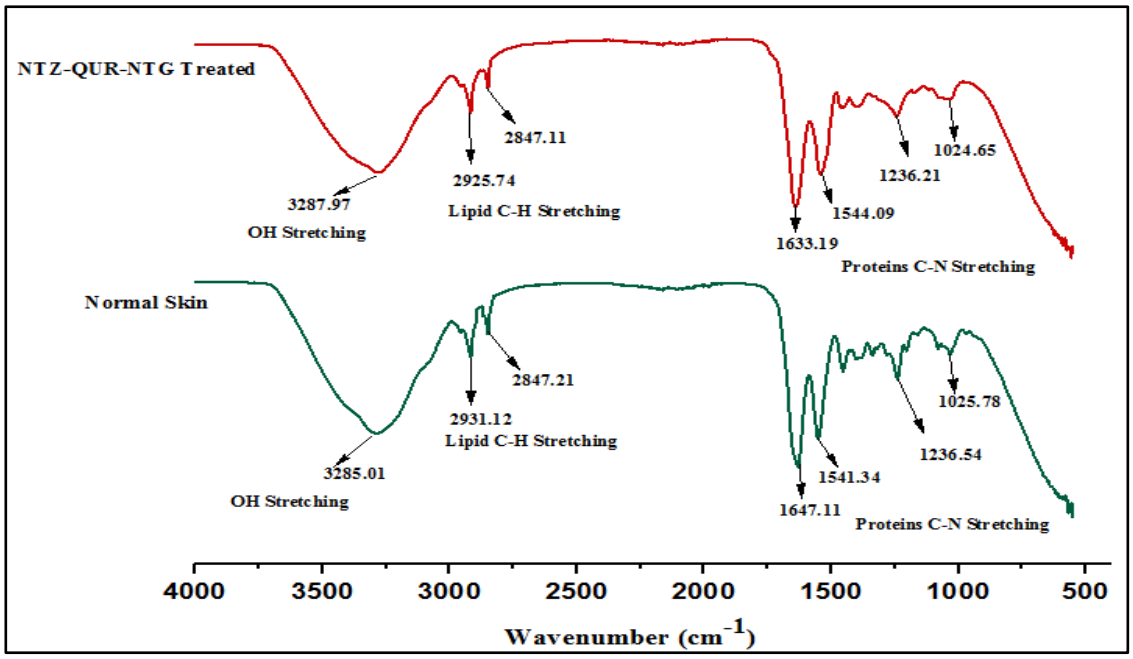

Figure 3.20. FTIR analysis of the NTZ-QUR-NTG treated skin and its comparison with normal skin

3.15. Skin Irritation and Histopathology Study

Draize scoring method was used for scoring in skin irritation test and results showed that NTZ-QUR-NTG was nonirritant as compared to control which is 0.8% formalin as depicted in **Table 3.12**. The histopathology investigation was carried out to confirm the Draize test and to evaluate the impact of NTZ-QUR-NTG on skin. No evidence of infiltration or loosened collagen fibers were found. Moreover, the epidermal layer was also found to be unaltered as shown in **Figure 3.21**. The outcomes were identical to what was seen with normal skin. However, damage to the epidermal layer and signs of infiltration were seen on skin treated with 0.8% formalin.

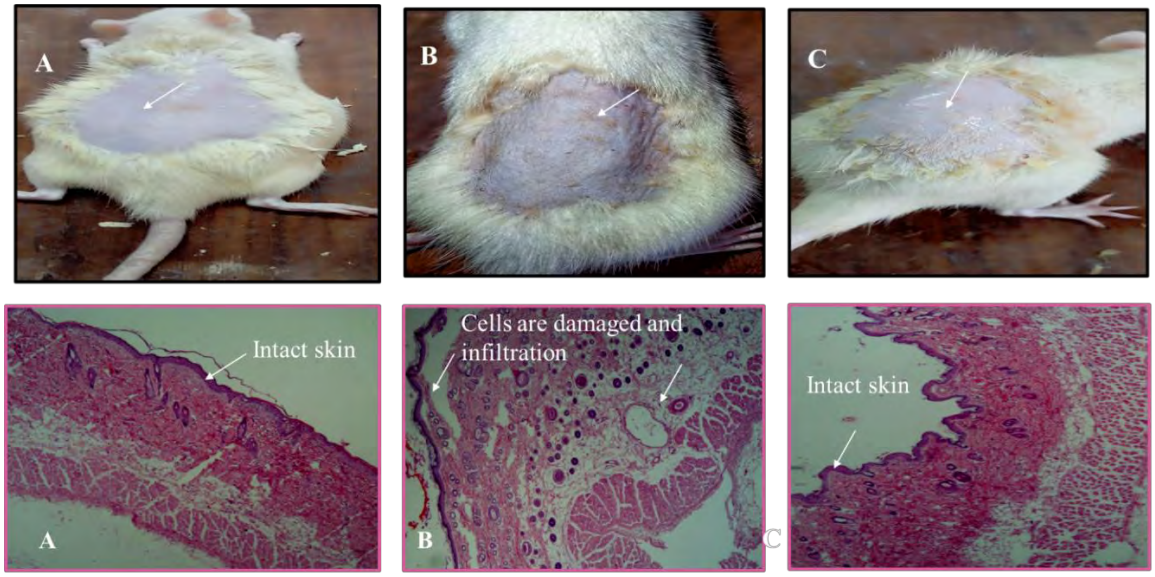

Figure 3.21. Normal skin **(A)**, 0.8% Formalin treated skin **(B)**, NTZ-QUR-NTG treated skin **(C)**

Table: 3.12. Draize scoring data for skin irritation test.

Groups	Erythema				Edema				PDII
	1 hr	24 hr	48 hr	72 hr	1 hr	24 hr	48 hr	72 hr	
Normal	0	0	0	0	0	0	0	0	0
Formalin treated (0.8%)	3	2	2	2	1	2	2	2	2
NTZ-QUR-NTG treated	0	0	0	0	0	0	0	0	0

Note: *PDII = Primary Dermal Irritation Index*

3.16. Qualitative Macrophage Uptake Study

The key obstacle to effective treatment is the inability of antileishmanial medications to enter macrophages. This was one of the main goals of the current study. A macrophage uptake test was conducted to achieve this goal. After 1 hr of incubation, intense internalized fluorescence was observed as shown in **Figure 3.24**, indicating passive targeting of macrophages by rhodamine loaded NT (Batool *et al.*, 2021). On the other hand, no fluorescence was seen in Rhodamine solution which was used as a control.

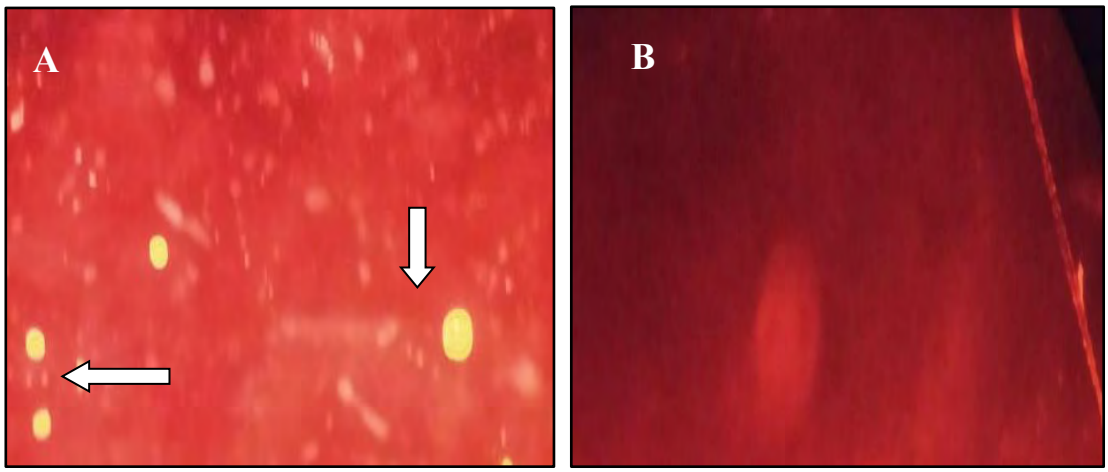

Figure 3.22. Macrophage uptake study: Rhodamine loaded NT treated macrophages **(A)**, Rhodamine solution treated macrophages **(B)**

3.17. Quantitative Macrophage Uptake Study

The quantitative macrophage uptake investigation was used to confirm the qualitative evaluation of macrophage internalization. The findings revealed that NTZ-QUR-NT were more up taken by macrophages. as 78.44 ± 0.95 µg of NTZ and 61.14 ± 1.23 µg of QUR from NTZ-QUR-NT were up taken by 2×10^4 macrophages. While in case of NTZ-QUR dispersion only 8.07 ± 1.19 µg of NTZ and 5.41 ± 1.54 µg of QUR were up taken by 2×10^4 macrophages.

Table 3.13. Quantitative data of uptake of NTZ and QUR by macrophages.

Sample	Quercetin (µg/2×10^4 macrophages)	Nitazoxanide (µg/2×10^4 macrophages)
NTZ-QUR-NT	61.14 ± 1.23	78.44 ± 0.95
NTZ-QUR dispersion	5.41 ± 1.54	8.07 ± 1.19

3.18. Cell Viability and Toxicity Assay

Cell viability assay was also carried out on macrophages previously collected from rat's abdominal cavity. After study it was found that cell viability percentage of NTZ-QUR-NT was higher at each concentration as compared to NTZ-QUR dispersion. Such as at concentration of 3.125 µg/ml 98% of cells were vial while in case of NTZ-QUR solution the viability of cells was 70%. The significant difference of both groups can be seen in **Figure 3.23**. NTZ-QUR-NT and NTZ-QUR dispersion CC_{50} values were

calculated by using GraphPad prism®. The result showed that NTZ-QUR-NT have 71.95 ± 3.32 CC_{50} value and NTZ-QUR dispersion have 49.77 ± 2.15 CC_{50}, which is indicating that NTZ-QUR-NT is safer to use as compared to NTZ-QUR dispersion.

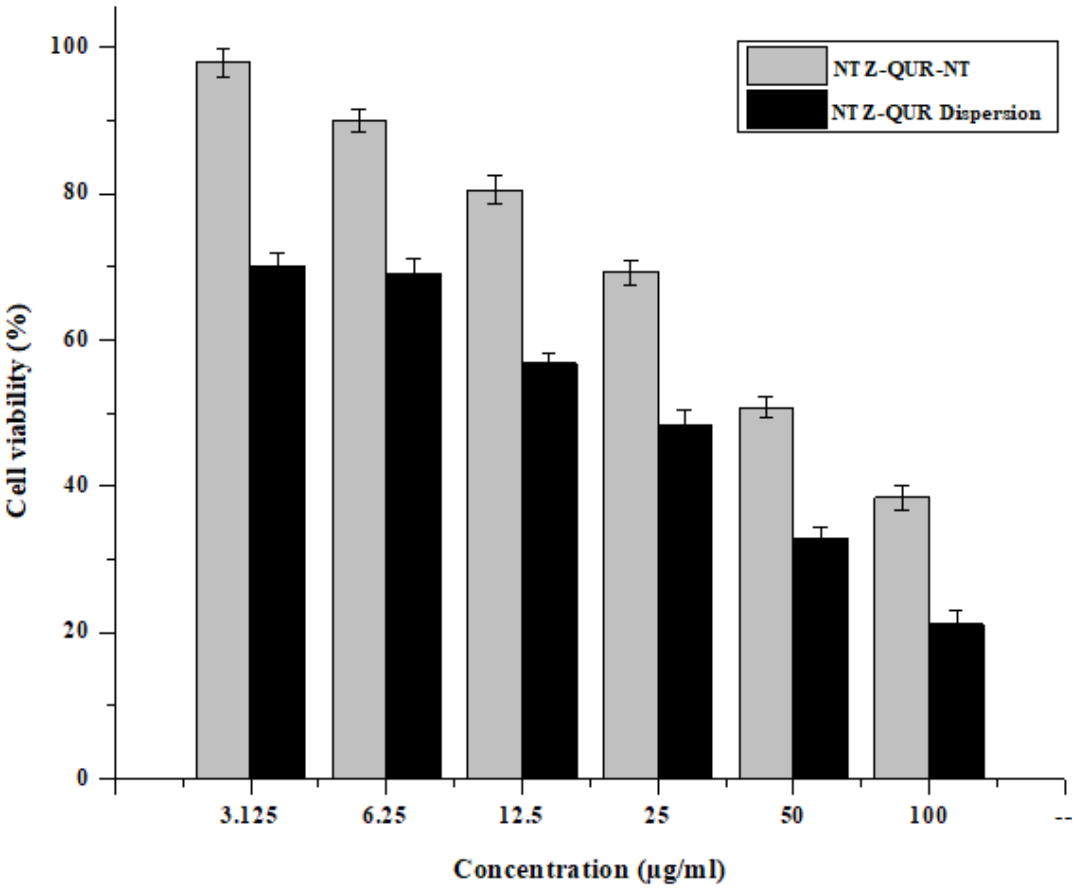

Figure 3.23. Cell viability assay of the NTZ-QUR-NT and NTZ-QUR dispersion

3.19. In-vitro Anti-leishmanial Activity Analysis Against *L. tropica*

The in-vitro anti-leishmanial assay was performed to check the IC_{50} value of NTZ-QUR-NT and to compare it with NTZ-NT, QUR-NT, NTZ dispersion, QUR dispersion and NTZ-QUR dispersion. IC_{50} values of NTZ and QUR dispersion alone were 29.67 ± 1.43 µg/ml and 43.72 ± 1.52 µg/ml, respectively. While the IC_{50} of NTZ and QUR in combination was 19.66 ± 1.17 µg/ml. The IC_{50} values of NTZ and QUR were reduced into 8.35 ± 0.95 µg/ml and 14.91 ± 1.09 µg/ml when separately loaded in NT. Moreover, the IC_{50} value was significantly reduced to 3.15 ± 0.89 µg/ml when the combination of both drugs was loaded into NT. The IC_{50} value of NTZ-QUR-NT against *L. tropica* promastigotes was 6.24-times lower than NTZ-QUR dispersion and

2.65 and 4.73-times as compared to NTZ-NT and QUR-NT respectively.

3.20. Determination of Combination Index (CI)

The reduced IC_{50} value of combination drugs may be due to the synergistic effect of both drugs which was confirmed by calculating the CI value, using Chou Talaly equation (Chou, 2010). The CI value of NTZ-QUR-NT was found to be 0.58 which showed synergistic interaction between both drugs loaded in NT.

CHAPTER 4

DISCUSSION

4. DISCUSSION

Although CL is the most prevalent type of leishmaniasis, it has received much less attention than visceral leishmaniasis (VL) (Dar, McElroy, *et al.*, 2020). Parenteral treatment for VL is effective in lowering parasite levels in the spleen and liver, but it has serious adverse effects and complications when used to treat CL (Jamshaid *et al.*, 2021). The liver and spleen's phagocytic cells may remove drug particles from systemic circulation, which reduce their availability at the sites of cutaneous infection where parasites reside. As a result, systemic medication delivery in CL is associated with considerable toxicity, requires careful monitoring, and nevertheless yields subpar outcomes (Shaw and Carter, 2014). Due to its non-invasiveness, the preparation of a topical formulations against CL is greatly desired, while ensuring medicine accessibility at the infection site. WHO highlights the search for new medications, drug repurposing, and combination therapy as initiatives to improve leishmaniasis treatment (World Health Organization, 2012). Numerous authors have emphasized the need of considering drug combinations in antileishmanial therapy as combination therapy is widely used for other infectious diseases, such as, AIDS, malaria and cancer (Bryceson, 2001; Olliaro, 2010). The combination therapy is thought to be the most successful and advantageous because it outperforms monotherapy even at much lower doses (Trinconi *et al.*, 2016).

Herein, the aim of our study was to passively target the leishmania parasites residing in macrophages of dermal layer of skin. For that purpose NTZ-QUR-NT were developed because NT have the ability to easily cross the SC due to their deformable nature and to reach the targeted dermal site (Ferreira *et al.*, 2004). Optimization of NTZ-QUR-NT was done by using BBD of software Design Expert®. Lipid (PL90G), surfactant (Tween® 80) and drug (QUR) were selected as independent variables while particle size, PDI, ZP and %EE were kept as dependent variables. The particle size and PDI of NTZ-QUR-NT were found to increase with increasing lipid content. This could be explained by the increase in densely packed vesicular lipid bilayers (Abdel Messih *et al*., 2017). Furthermore, as previously reported, the increase in lipid concentration may result in the development of multilamellar vesicles with larger diameters (Ahmed, 2015). In contrast, higher Tween® 80 concentrations in NTZ-QUR-NT led to smaller particles, probably as a result of lower interfacial tension (Salim *et al.*, 2020; Batool *et al.*, 2021). The value ZP was increased by increasing the concentration of PL90G. The

negatively charged PL90G molecules, which create the vesicles with binary lipid layers, are thought to be the cause of NTZ-QUR-NT negative ZP. The value of ZP was decreased with surge in Tween® 80 concentration. Considering Tween® 80's increased surface activity, the result implied that it did adsorb on the particle surfaces by displacing the endogenous surface active molecules (Witayaudom and Klinkesorn, 2017). As it is a nonionic surfactant, a decrease in net charge at the particle surface was attributed to increase in its adsorption on the surface of NTZ-QUR-NT (Kheradmandnia *et al.*, 2010). In NTZ-QUR-NT the entrapment of both QUR and NTZ were found to be significantly increased by increasing lipid concentration. The increase in lipid concentration enhances the drug's solubilization and so create more space where more drug molecules can fit, may be responsible for the increase in entrapment (Shah and Pathak, 2010). The %EE of both drugs were reduced when the surfactant concentration increased. Because surfactant aligns in the lipid bilayer similarly to lipophilic drugs and competes with them for space, which lead to the decrease in the amount of entrapment (Dar, McElroy, *et al.*, 2020). With an acceptable particle size (210.90 ± 3.67 nm) and a low PDI (0.155 ± 0.009), NT-3 formulation was suggested as optimized from the **Table 3.5**, which also showed good particles segregation and stability with high entrapment of NTZ and QUR. Particles less than 100 nm are not ideal for this formulation because they frequently manage to avoid being up taken by macrophages. On the other side, less than 300 nm is the optimal particle size to penetrate the stratum corneum (Dar, Khalid, *et al.*, 2020).

Single-layered spherical morphology and nano-size range of NTZ-QUR-NT were also confirmed by TEM analysis. The NTZ-QUR-NT deformability index, which was found to be 0.9264 ± 0.042, was used to determine the deformation and stress-induced transformation capabilities of trans. Tween® 80, a surfactant that serves as an edge activator, may be responsible for the high deformability index value. Because of its long, light, and highly malleable carbon chain, it has a high degree of deformability (El Zaafarany *et al.*, 2010). No physical and chemical interactions were found between components of NTZ-QUR-NT after FTIR analysis. Chitosan gel that was loaded with NTZ-QUR-NT undergone physicochemical investigation. The pH, color, homogeneity, and viscosity of the gel was analyzed. The gel was seen to be opaque, uniform in texture, and yellow in color. The gel's pH was 5.8 ± 1.56, which is within 4-6, the usual range for the pH of skin (Lambers *et al.*, 2006; Verma and Pathak, 2012). High

spreadability and faster dissemination are characteristics of an excellent gel .The NTZ-QUR-NTG exhibited spreadability of 310.50 ± 3.5%, which was easy to spread (Ahad *et al.*, 2016). Rheological investigation of NTZ-QUR-NTG indicated, a decrease in gel viscosity with escalation in shear rate. The term "non-newtonian" refers to this behavior, and gels that display it are referred as "shear thinning gels." Such behavior, according to studies, is desirable when applying gel to the skin (Li *et al.*, 2003; Kaura *et al.*, 2015).

In-vitro release study was performed on physiological pH of skin macrophages endosomes (5.5) and blood (7.4) to assess the release pattern of both drugs NTZ and QUR. The results showed that almost 85% and 90% of the NTZ and QUR were released from dispersion in first 4 hrs while in case of our designed formulations NTZ-QUR-NT and NTZ-QUR-NTG sustain the release of both drugs up to 24 hrs. The sustain release of drugs would prevent the need of frequent dosing. Initially the release of both drug from NTZ-QUR-NT was burst likely due to drugs un-entrapment or desorption from the surface of the vesicles. Later, though, the release slowed, indicating a sustained release pattern. The release of NTZ and QUR is significantly lower ($p < 0.05$) from NTZ-QUR-NTG as compared to dispersions. This is because in case of NTG the drugs must pass through two barriers: first, it must be released from the NT and then it must pass through the chitosan gel (Dar *et al.*, 2018). QUR release from QUR dispersion was more in pH 7.4 as compared to pH 5.5 due to its acidic nature as it more solubilize in basic media (Gaohua *et al.*, 2021). Furthermore, as previously reported, the media's neutral or acidic pH had no significant impact on the drugs release from the NT and NTG (Want *et al.*, 2017).

To analyze the release mechanism of QUR and NTZ from transferosomes and transferosomal gel different kinetic models (First order, zero order, Korsmeyer-Peppas, Hixon-Crowell, first order, Higuchi) were applied by utilizing DD-solver (Microsoft Excel Add-in). By analyzing R^2 values of all models Korsmeyer-Peppas was considered as most fitting for release of both drugs from NT and Higuchi form NTG. The value of diffusion exponent (n) is considered key factor in release kinetic study, which is used to confirm that whether the release of drugs from drug delivery system is fickian or non-fickian diffusion (Ritger and Peppas, 1987). As the values of were less than 0.45 in cases NTZ-QUR-NT and greater than 0.45 in case of NTZ-QUR-NTG which

suggested that the release of QUR and NTZ was through fickian diffusion from NT and non-fickian from NTG.

The ex-vivo permeation study, which quantifies the amount of drug available to the body, offers vital information about the NTZ-QUR-NT behavior in in-vivo setting. The key mechanism of NT skin permeation into the SC and deeper skin layer is because of the trans-epidermal osmotic gradient. The NTZ-QUR-NT experience no more water influx gradient when they reach the moist viable epidermis which retards their further movement (Gupta *et al.*, 2012). This function is very important for enhancing skin retention of drugs at the infection site for a longer period of time and aids in minimizing the systemic toxicity (Dar, McElroy, *et al.*, 2020). In the current investigation, it was discovered that drug retention in deeper skin layers was higher than drug permeation, which is helpful for the topical therapy of CL since more retention than permeability is needed.

The stability and fluidity of the lipids present in the skin, especially in the SC, are altered by various polymeric nanoparticles and liposomes as they move through the skin (Zeb *et al.*, 2016). Thus, skin FTIR analysis was used to examine that how NT would affect the lipids in the skin layers. The FTIR spectra demonstrated that NTZ-QUR-NT have no detrimental effects on skin structures, and it was determined that their penetration through upper skin layers was caused by their capability to transform shape (Rabia *et al.*, 2020). Any dosage form intended for topical application to the skin should be non-toxic and non-irritating. A skin irritation investigation using NTZ-QUR-NTG was conducted to verify safety, and the results were compared to those for conventional formalin (Kumbhar *et al.*, 2013). The NTZ-QUR-NTG offers a better safety profile, as shown by this investigation. The results of the skin irritation test were also supported by a histopathology analysis, which found that the NTZ-QUR-NTG did not damage any tissues or result in any inflammation.

Since the parasites reside inside the macrophages, the effectiveness of an anti-leishmanial formulation mainly relies on how well it targets and accumulates there (Shahnaz *et al.*, 2017). According to the findings of the qualitative uptake investigation, dye loaded NT were endocytosed after 30 min of incubation, and the cytosol of PMs displayed high intracellular fluorescence. The quantitative macrophage uptake investigation was used to confirm the qualitative evaluation of macrophage

internalization. In comparison to NTZ-QUR dispersion, NTZ-QUR-NT cell internalization was almost 10-folds higher. It was clear from result that NTZ-QUR dispersion was distributed rather than particularly internalized by macrophages. Due to favorable vesicle characteristics and successful localization of nanocarriers in the infected macrophages, which is the preferred site of action for anti-leishmanial drugs, it was anticipated that NTZ and QUR anti-leishmanial efficacy and potential could be significantly improved when entrapped within NT (Treiger Borborema *et al.*, 2011). Furthermore, internalization of drug-loaded NT in macrophages may make them act like a secondary drug depot, improving drug availability to parasites that live inside them (Moosavian Kalat *et al.*, 2014).

Synergistic interaction was found between QUR and NTZ against *L. tropica* amastigotes. QUR shows its anti- leishmanial effect by inhibiting the arginase enzyme which is important for parasite proliferation (Sousa-Batista *et al.*, 2017). It also causes the mitochondrial damage of parasite by increasing ROS level (Gervazoni *et al.*, 2020). QUR has been purposed as potential candidate in combination with other antileishmanial agents for treatment of cutaneous leishmaniasis (Sarkar *et al.*, 2002). NTZ is a broad spectrum antiparasitic drug which shows its anti-leishmanial action by inhibiting the pyruvate ferredoxin oxidoreductase (PFOR) which play critical role in energy metabolism of parasites (Assays and Leishmania, 2021). Combination index and antileishmanial activity of NTZ and QUR was further improved when both drugs were loaded in NT. The in-vitro anti-leishmanial assay indicated that the IC_{50} of NTZ-QUR-NT were 6.24-times lowered than NTZ-QUR dispersion. NTZ-QUR-NT were found more effective mainly because of their nano range size, ultra-deformable nature and high macrophage internalization (Zeb *et al.*, 2016; Dar *et al.*, 2018). Additionally, the vesicle's expressed negative charge made it ideal for targeting parastito-phorous vacuoles, an intra-macrophagial parasite home (Tempone *et al.*, 2004).

CONCLUSIONS

- NTZ-QUR-NT were successfully developed, optimized, and loaded into a chitosan-based gel for topical application. The optimized formulation had particles in nano-size range, low PDI, adequate drug entrapment and good deformability. No physical and chemical interactions were found between components of NTZ-QUR-NT.
- Both the drugs showed sustained release from NTZ-QUR-NT and NTZ-QUR-NTG, although the drug release from NTG was significantly different. Significant amount of the drugs was observed to be retained in the deeper skin layers after application of the formulation, an indication to the antileishmanial system's effectiveness.
- In vivo skin irritation and histopathological findings did not show any topical irritation associated with NTZ-QUR-NTG. Moreover, macrophage uptake analysis demonstrated that NTZ-QUR-NT were able to enhance macrophage internalization of both the drugs by passive targeting.
- Upon assessment in terms of anti-leishmanial potential, cell viability and toxicity the NTZ-QUR-NT system was found superior to NTZ-QUR dispersion. Overall, it is concluded that the NTZ-QUR-NTG has the ability to passively target the macrophages residing in the dermal layer with improved anti-leishmanial effect

FUTURE PROSPECTIVES

- In order to find the extent of permeation of transferosomes into deeper skin layers, fluorescent microscopy can be performed for skin treated with dye loaded transferosomes.
- In-vivo anti-leishmanial assay must be performed to properly assess the therapeutic response of this designed co-loaded nano system (NTZ-QUR-NT).
- Different ligands can be attached to NTZ-QUR-NT for more advanced and active targeting of the leishmanial parasites.

REFERENCE

REFERENCES

Abadias GI, Diago A, Cerro PA, Palma RAM and Gilaberte Y (2021). Cutaneous and Mucocutaneous Leishmaniasis. Actas Dermosifiliogr, 112(7): 601–618.

Agrahari V and Mitra AK (2016). Conventional formulations and emerging delivery systems for the topical treatment of Cutaneous Leishmaniasis. Ther Deliv, 7(2): 117–138.

Ahad A, Aqil M, Kohli K, Sultana Y and Mujeeb M (2015). The ameliorated longevity and pharmacokinetics of valsartan released from a gel system of ultradeformable vesicles. Ther Deliv, 44(6): 1457-1463.

Ahmed TA (2015). Preparation of transfersomes encapsulating sildenafil aimed for transdermal drug delivery : Plackett – Burman design and characterization. J Liposome Res, 25(1): 1–10.

Awabreh A, Schoenian G, Hamarsheh O and Presber W (2006). Clinical diagnosis of cutaneous leishmaniasis: A comparison study between standardized graded direct microscopy and ITS1-PCR of Giemsa-stained smears. Acta Trop, 99(1): 55–61.

Alam S, Panda JJ and Chauhan VS (2012). Novel dipeptide nanoparticles for effective curcumin delivery. Int J Nanomedicine, 7: 4207–4222.

Alvar J, Velez ID, Bern C, Herrero M, Desjeux P, Cano J, Jannin J and de Boer M (2012). Leishmaniasis worldwide and global estimates of its incidence. PLoS ONE, 7(5): 35671.

Alvar J, Yactayo S and Bern C (2006). Leishmaniasis and poverty. Trends Parasitol, 22(12): 552–557.

Alvi IA, Madan J, Kaushik D, Sardana S, Pandey RS and Ali A (2011). Comparative study of transfersomes, liposomes, and niosomes for topical delivery of 5-fluorouracil to skin cancer cells: Preparation, characterization, in-vitro release, and cytotoxicity analysis. Anticancer Drugs, 22(8): 774–782.

Anderson VR and Curran MP (2007). Nitazoxanide: a review of its use in the treatment of gastrointestinal infections. Drugs, 67(13): 1947–1967.

Andrade-neto VV, Cunha-junior EF, Faioes S, Pereira T, Silva RL, Leon LL and Torres-santos EC (2018). Leishmaniasis treatment: update of possibilities for drug repurposing. Front Biosci, 23(5): 967–996.

Apsara S, Opatha T, Titapiwatanakun V and Chutoprapat R (2020). Transfersomes : A Promising Nanoencapsulation Technique for Transdermal Drug Delivery. Pharmaceutics, 12(9): 855.

Aishah EA, Hamdan IA, Amal KK, Abdullah DA, Ali M, Massumeh N and Hossein M (2021). The Potential Use of Nitazoxanide in the Treatment of Cutaneous The Potential Use of Nitazoxanide in the Treatment of Cutaneous Leishmaniasis : In-Vitro Assays Against Leishmania Tropica. Int J Pharm Res, 14(3): 1451.

Avadhani KS, Manikkath J, Tiwari M, Godavarthi A, Vidya SM, Raghu C, Kalthur G, Udupa N, Avadhani KS, Manikkath J, Tiwari M, Chandrasekhar M and Godavarthi A (2017). Skin delivery of epigallocatechin-3-gallate (EGCG) and hyaluronic acid loaded nano-transfersomes for antioxidant and anti-aging effects in UV radiation induced skin damage loaded nano-transfersomes for antioxidant and anti-aging effects. Drug Deliv, 24(1): 61-74.

Bailey MS (2011). Cutaneous leishmaniasis in British troops following jungle training in Belize. Travel Med Infect Dis, 9(5): 253–254.

Baileyid F, Mondragon-Shem, K, Haines LR, Olabi A, Alorfi A, Ruiz-Postigo JA, Alvar J, Hotez P, Adams ER, Vélez ID, Al-Salem W, Eaton J, Acosta-Serrano Á and Molyneux DH (2019). Cutaneous leishmaniasis and co-morbid major depressive disorder: A systematic review with burden estimates. PLOS Negl Trop Dis, 13(2): 1–22.

Balata GF, Faisal MM, Elghamry HA and Sabry SA (2020). Preparation and Characterization of Ivabradine HCl Transfersomes for Enhanced Transdermal Delivery. J Drug Deliv Sci Technol, 60: 101921.

Bamorovat M, Sharifi I, Mohammadi MA, Eybpoosh S, Nasibi S, Aflatoonian MR and Khosravi A (2018). Leishmania tropica isolates from non-healed and healed patients in Iran: A molecular typing and phylogenetic analysis. Microb Pathog, 116: 124–129.

Barry BW (2004). Breaching the skin's barrier to drugs. Nat Biotechnol, 22(2): 165–167.

Batool S, Zahid F, Ud-Din F, Naz SS, Dar MJ, Khan MW, Zeb A and Khan GM (2021). Macrophage targeting with the novel carbopol-based miltefosine-loaded transfersomal gel for the treatment of cutaneous leishmaniasis: in vitro and in vivo analyses. Drug Dev Ind Pharm, 47(3): 440–453.

Briones NCA, Cid AG, Romero AI, García-Bustos MF, Villegas M and Bermúdez JM (2021). An appraisal of the scientific current situation and new perspectives in the treatment of cutaneous leishmaniasis. Acta Trop, 221(5): 105988.

Bryceson A (2001). A policy for leishmaniasis with respect to the prevention and control of drug resistance. Trop Med Int Health, 6(11): 928–934.

Carvalho de, LMV, Pimentel MIF, Conceição-Silva F, e Vasconcellos É de CF, Valete-Rosalino CM, Lyra MR, Salgueiro M de M, Saheki MN, Madeira M de F, Mouta-Confort E, Antonio L de F, da Silva AF, Quintella LP, Bedoya-Pacheco SJ and Schubach A de O (2017). Sporotrichoid leishmaniasis: A cross-sectional clinical, epidemiological and laboratory study in Rio de Janeiro State, Brazil. Rev Inst Med Trop, 59: 33

Cevc G and Blume G (2001). New, highly efficient formulation of diclofenac for the topical, transdermal administration in ultradeformable drug carriers, Transfersomes. Biochim Biophys, 1514(2): 191–205.

Cevc G and Scha A (2002). Ultradeformable lipid vesicles can penetrate the skin and other semi-permeable barriers unfragmented . Evidence from double label CLSM experiments and direct size measurements. Biochim Biophys Acta, 1564: 21–30.

Chan-Bacab MJ, Hernandez-Nunez E and Navarrete-Vázquez G (2009). Nitazoxanide, tizoxanide and a new analogue [4-nitro-N-(5-nitro-1,3- thiazol-2-yl)benzamide; NTB] inhibit the growth of kinetoplastid parasites (Trypanosoma cruzi and Leishmania mexicana) in vitro. J Antimicrob Chemo 63(6): 1292–1293.

Chou TC (2010). Drug combination studies and their synergy quantification using the chou-talalay method. Cancer Res, 70(2): 440–446.

Christensen SM, Belew AT, El-Sayed NM, Tafuri WL, Silveira FT and Mosser DM (2018). Host and parasite responses in human diffuse cutaneous leishmaniasis caused by L. amazonensis. PLoS Negl Trop, 13(3): 1–23.

Dar MJ, McElroy CA, Khan MI, Satoskar AR and Khan GM (2020). Development and evaluation of novel miltefosine-polyphenol co-loaded second generation nano-transfersomes for the topical treatment of cutaneous leishmaniasis. Expert Opin Drug Deliv, 17(1): 97–110.

Dar MJ, Khalid S, Varikuti S, Satoskar AR and Khan GM (2020). Nano-elastic liposomes as multidrug carrier of sodium stibogluconate and ketoconazole: A potential new approach for the topical treatment of cutaneous Leishmaniasis. Eur J Pharm Sci, 145: 105256.

Dar MJ, Din FU and Khan GM (2018). Sodium stibogluconate loaded nano-deformable liposomes for topical treatment of leishmaniasis : macrophage as a target cell. Drug Deliv, 25(1): 1595–1606.

Desjeux P (2004). Leishmaniasis: Current situation and new perspectives. Comp Immunol Microbi, 27(5): 305–318..

Din FU, Rashid R, Mustapha O, Kim DW, Park JH, Ku SK, Oh YK., Kim J.O, Youn YS, Yong CS and Choi HG (2015). Development of a novel solid lipid nanoparticles-loaded dual-reverse thermosensitive nanomicelle for intramuscular administration with sustained release and reduced toxicity. RSC Adv, 5(54): 43687–43694.

Dubey V, Mishra D, Nahar M and Jain NK (2007). Vesicles as tools for the modulation of skin permeability**.** Expert Opin Drug Deliv, 4(6)579–594.

Emamzadeh M, Desmaële D, Couvreur P and Pasparakis G. (2018). Dual controlled delivery of squalenoyl-gemcitabine and paclitaxel using thermo-responsive polymeric micelles for pancreatic cancer. J Mater Chem B, 6(15): 2230–2239.

Fernández-García R, Lalatsa A, Statts L, Bolás-Fernández F, Ballesteros MP and Serrano DR (2020a). Transferosomes as nanocarriers for drugs across the skin: Quality by design from lab to industrial scale. Int J Pharm, 573: 118817.

Fernández-García R, Lalatsa A, Statts L, Bolás-Fernández F, Ballesteros MP and Serrano DR (2020b). Transferosomes as nanocarriers for drugs across the skin: Quality by design from lab to industrial scale. Int J Pharm, 573: 118817.

Ferreira LS, Ramaldes GA, Nunan EA and Ferreira LAM (2004). In Vitro Skin Permeation and Retention of Paromomycin from Liposomes for Topical Treatment of the Cutaneous Leishmaniasis. Drug Dev Ind Pharm, 30(3): 289–296.

Firake BM, Chettiar R and Firake TB (2017). Nitazoxanide : A Review of Analytical Methods. Pharma Tutor, 5(9), pp. 61–68.

Gao W, Zhang Y, Zhang Q and Zhang L (2016). Nanoparticle-Hydrogel: A Hybrid Biomaterial System for Localized Drug Delivery. Ann Biomed Eng, 44(6): 2049–2061.

Gao Y, Wang Y, Ma Y, Yu A, Cai F, Shao W and Zhai G (2009). Colloids and Surfaces B : Biointerfaces Formulation optimization and in situ absorption in rat intestinal tract of quercetin-loaded microemulsion. Colloids Surf. B, 71(2): 306–314.

Gaohua L, Miao X and Dou L (2021). Crosstalk of physiological pH and chemical pKa under the umbrella of physiologically based pharmacokinetic modeling of drug absorption, distribution, metabolism, excretion, and toxicity. Expert Opin Drug Metab, 17(9): 1103–1124.

Gervazoni LFO, Barcellos GB, Ferreira-Paes T. and Almeida-Amaral EE (2020). Use of Natural Products in Leishmaniasis Chemotherapy: An Overview. Front Chem, 8: 1–43.

Gracielle E, Barbosa LRS, Mortara RA and Gustavo A (2020). Chemico-Biological Interactions entrapped into phosphatidylserine-nanoliposomes : An experimental study. Chem Biol Interact, 332: 109296..

Gupta A, Aggarwal G, Singla S and Arora R (2012). Transfersomes: A novel vesicular carrier for enhanced transdermal delivery of sertraline: Development, characterization, and performance evaluation. Sci Pharm, 80(4): 1061–1080.

Gurgen J, Hogan D, Grace E. and Johnson D (2011). Nitazoxanide in the treatment of chronic cutaneous leishmaniasis resistant to traditional sodium stibogluconate. J Am Acad Dermato, 64(1): 202–203.

Hanaa AAM, Rania AHI, Ahmed SG and Mansour S (2017). Nanoethosomes for Transdermal Delivery of Tropisetron HCl: Multi-factorial predictive modeling, characterization and ex-vivo skin permeation. Drug Dev Ind Pharm, 43(6): 958-971.

Henrique A, Cataneo D, Tomiotto-pellissier F, Miranda-sapla MM, Paulo J, Panis C, Kian D, Megumi L, Simão ANC, Casagrande R, Pinge-filho P, Nazareth I, Varri WA Jr and Conchon-costa I (2019). Biomedicine & Pharmacotherapy Quercetin promotes antipromastigote e ff ect by increasing the ROS production and anti-amastigote by upregulating Nrf2/HO-1 expression, affecting iron availability. Biomed. Pharmacother, 113: 108745.

Jamshaid H, Din FU and Khan GM (2021). Nanotechnology based solutions for anti-leishmanial impediments: a detailed insight. J Nanobiotechnology, 19(1): 1–51.

Jangdey MS, Gupta A, Saraf Shailendra and Saraf Swarnlata (2017). Development and optimization of apigenin-loaded transfersomal system for skin cancer delivery: in vitro evaluation. Artif Cells Nanomed Biotechnol, 45(7): 1452–1462.

Jr ACW (2004). Nitazoxanide: a new broad spectrum antiparasitic agent**.** Expert Rev Anti Infect Ther, 2(1): 43-49.

Kang MJ, Eum JY, Jeong MS, Choi SE, Park SH., Cho HI, Cho CS, Seo SJ, Lee MW and Choi YW (2010). Facilitated skin permeation of oregonin by elastic liposomal

formulations and suppression of atopic dermatitis in NC/Nga mice. Biol Pharm Bull, 33(1): 100–106.

Kaura L, Subheet KJ and Singh K. (2015). Vitamin E TPGS based nanogel for skin targeting of high molecular weight anti-fungal drug: Development, in vitro and in vivo assessment. RSC Adv, (66).

Khaleeq N, Din FU, Khan AS, Rabia S, Dar J and Khan GM (2020). Development of levosulpiride-loaded solid lipid nanoparticles and their in vitro and in vivo comparison with commercial product.J Microencapsul, 37(2): 160–169.

Khan AS, ud Din FU, Ali Z, Bibi M, Zahid F, Zeb A, Mujeeb-ur-Rehman and Khan GM (2021). Development, in vitro and in vivo evaluation of miltefosine loaded nanostructured lipid carriers for the treatment of Cutaneous Leishmaniasis. Int J Pharm., 593: 120109.

Khan NH, Bari AU, Hashim R, Khan I, Muneer A, Shah A, Wahid S, Yardley V, O'Neil B and Sutherland CJ (2016). Cutaneous leishmaniasis in Khyber Pakhtunkhwa province of pakistan: Clinical diversity and species-level diagnosis. Am J Trop Med Hyg, 95(5): 1106–1114.

Kheradmandnia S, Vasheghani-Farahani E, Nosrati M and Atyabi F (2010). Preparation and characterization of ketoprofen-loaded solid lipid nanoparticles made from beeswax and carnauba wax. Nanomed.: Nanotechnol Biol Med, 6(6): 53–759.

Kumbhar D, Wavikar P and Vavia P (2013) Niosomal gel of lornoxicam for topical delivery: In vitro assessment and pharmacodynamic activity. AAPS PharmSciTech, 14(3). 1072–1082.

Lambers H, Piessens S, Bloem A, Pronk H and Finkel P (2006). Natural skin surface pH is on average below 5, which is beneficial for its resident flora. Int J Cosmet Sci, 28(5): 359–370.

Rossignol JF (2014). Nitazoxanide : A first-in-class broad-spectrum antiviral agent. Antiviral Res, 110: 94-103.

Li J, Ni X and Leong KW (2003). Injectable drug-delivery systems based on supramolecular hydrogels formed by poly(ethylene oxide)s and α-cyclodextrin. J Biomed Mater Res, 65(2): 196–202.

Laxmi MV, Zafaruddin M and Kuchana V (2015). Design and Characterization of Transferosomal Gel of Repaglinide. Int Res J Pharm, 6(1): 38–42.

El Maghraby GMM, Williams AC and Barry BW (2010). Skin hydration and possible shunt route penetration in controlled estradiol delivery from ultradeformable and standard liposomes. J Pharm Pharmacol, 53(10): 1311–1322.

Mahajan HS (2018). Quercetin Loaded Nanostructured Lipid Carriers for Nose to Brain Delivery : In Vitro and In Vivo Studies. Adv Drug Deliv Rev, 6: 9–20.

Marques MJ, Volpini ÂC, Machado-Coelho GLL, Machado-Pinto J, Da Costa CA, Mayrink W, Genaro O and Romanha AJ (2006). Comparison of polymerase chain reaction with other laboratory methods for the diagnosis of American cutaneous leishmaniasis: Diagnosis of cutaneous leishmaniasis by polymerase chain reaction.

Diagn Microbiol Infect, 54(1): 37–43.

Maurya PK (2022). Health Benefits of Quercetin in Age-Related Diseases. Molecules, 27(8): 2498.

Mehwish S, Khan H, Rehman AU, Khan AU, Khan MA, Hayat O, Ahmad M, Wadood A and Ullah N (2019). Natural compounds from plants controlling leishmanial growth via DNA damage and inhibiting trypanothione reductase and trypanothione synthetase: an in vitro and in silico approach. Biotech, 9(8): 1–14.

Minodier P and Parola P (2007). Cutaneous leishmaniasis treatment. Travel Med Infect Dis, 5(3): 150–158.

Moosavian KSA, Khamesipour A, Bavarsad N, Fallah M, Khashyarmanesha Z, Feizi E, Neghabi K, Abbasi A and Jaafari MR (2014). Use of topical liposomes containing meglumine antimoniate (Glucantime) for the treatment of L. major lesion in BALB/c mice. Exp. Parasitol, 143(1): 5–10.

Nazari-Vanani R, Vais RD, Sharifi F, Sattarahmady N, Karimian K, Motazedian MH and Heli H (2018). Investigation of anti-leishmanial efficacy of miltefosine and ketoconazole loaded on nanoniosomes. Acta Trop, 185: 69–76.

Olliaro PL (2010). Drug combinations for visceral leishmaniasis, Curr Opin Infect Dis, 23(6): 595–602.

Rothwell JA, Day AJ, Morgan MR (2005). Experimental Determination of Octanol − Water Partition Coefficients of Quercetin and Related Flavonoids. J Agric Food Chem, 53(11): 4355-60.

Oryan A (2015). Plant-derived compounds in treatment of leishmaniasis. Iran J Vet Res, 16(1): 1–19.

Pal C and Bandyopadhyay . (2012). Redox-Active Antiparasitic Drugs. Antioxid. Redox Signal, 17(4).

Pourmohammadi B, Motazedian M, Hatam G, Kalantari M, Habibi P and Sarkari B (2010). Comparison of three methods for diagnosis of cutaneous leishmaniasis. Iran J Parasitol, 5(4): 1–8.

Psimadas D, Georgoulias P, Valotassiou V and Loudos G (2012). Molecular Nanomedicine Towards Cancer. Pharm Sci, 101(7): 2271–2280.

Rabia S, Khaleeq N, Batool S, Dar MJ, Kim DW, Din FU and Khan GM (2020). Rifampicin-loaded nanotransferosomal gel for treatment of cutaneous leishmaniasis: Passive targeting via topical route. Nanomedicine, 15(2): 183–203.

Rasti S, Ghorbanzadeh B, Kheirandish F, Mousavi SG, Pirozmand A, Hooshyar H and Abani B (2016). Comparison of Molecular , Microscopic , and Culture Methods for Diagnosis of Cutaneous Leishmaniasis. J Clin Lab Anal,(5): 6–10.

Reithinger R and Dujardin JC (2007). Molecular diagnosis of leishmaniasis: Current status and future applications. J Clin Microbiol, 45(1): 21–25.

Riaz A, Ahmed N, Khan MI, Haq I, Rehman A and Khan GM (2019). Formulation of

topical NLCs to target macrophages for cutaneous leishmaniasis. J Drug Deliv Sci Technol, 54: 101232.

Ritger PL and Peppas NA (1987). A Simple Equation For Description Of Solute Release. J Control. Release, 5: 23–36.

Salama AH and Aburahma MH (2016).Ufasomes nano-vesicles-based lyophilized platforms for intranasal delivery of cinnarizine: preparation, optimization, ex-vivo histopathological safety assessment and mucosal confocal imaging. Pharm Dev Technol, 21(6): 706–715.

Salim MW, Shabbir K, Din FU, Yousaf AM, Choi HG and Khan GM (2020). Preparation, in-vitro and in-vivo evaluation of Rifampicin and Vancomycin Co-loaded transfersomal gel for the treatment of cutaneous leishmaniasis. J Drug Deliv Sci Technol, 60; 101996.

Sarkar S, Mandal S, Sinha J, Mukhopadhyay S, Das N and Basu MK (2002). Quercetin: Critical evaluation as an antileishmanial agent in vivo in hamsters using different vesicular delivery modes. J Drug Target, 10(8): 573–578.

Scott P and Novais FO (2016). Cutaneous leishmaniasis: Immune responses in protection and pathogenesis. Nat Rev Immunol, 16(9): 581–592.

Shah M and Pathak K (2010). Development and statistical optimization of solid lipid nanoparticles of simvastatin by using 23 full-factorial design. AAPS PharmSciTech, 11(2): 489–496.

Shah R, Eldridge D, Palombo E and Harding I (2014). Optimisation and stability assessment of solid lipid nanoparticles using particle size and zeta potential. J Phys Sci, 25(1): 59–75.

Shahnaz G, Edagwa BJ, McMillan J, Akhtar S, Raza A, Qureshi NA, Yasinzai M and Gendelman HE (2017). Development of mannose-anchored thiolated amphotericin B nanocarriers for treatment of visceral leishmaniasis. Nanomedicine, 12(2): 99–115.

Sharma L, Dhiman M, Singh A and Sharma MM (2021). Green Approach: A Forwarding Step for Curing Leishmaniasis—A Neglected Tropical Disease. Front Mol Biosci, 8: 655584.

Sharma V, Yusuf M and Pathak K (2014). Nanovesicles for transdermal delivery of felodipine: Development, characterization, and pharmacokinetics. Int J Pharm Investig, 4(3): 119.

Shaw CD and Carter KC (2014). Drug delivery: Lessons to be learnt from Leishmania studies. Nanomedicine, 9(10): 1531–1544.

Simeonov A, Jadhav A, Sayed AA, Wang Y, Nelson ME, Thomas CJ, Inglese J, Williams DL and Austin CP (2008). Quantitative High-Throughput Screen Identifies Inhibitors of the Schistosoma mansoni Redox Cascade. PLoS Negl Trop Dis, 2(1): 127

Sohrabi S, Haeri A, Mahboubi A, Mortazavi A and Dadashzadeh S (2016). Chitosan gel-embedded moxifloxacin niosomes: An efficient antimicrobial hybrid system for burn infection. Int. J Biol Macromol, 85: 625–633.

Sood S, Maddiboyina B, Rawat P, Garg AK, Foudah I, Alam A, Aldawsari HM, Riadi Y and Singh S (2020). Enhancing the solubility of nitazoxanide with solid dispersions technique : formulation , evaluation , and cytotoxicity study. J Biomater Sci Polym Ed, 32 (4): 1–11.

Sousa-Batista AJ, Poletto FS, Philipon CIMS, Guterres SS, Pohlmann AR and Rossi-Bergmann B (2017). Lipid-core nanocapsules increase the oral efficacy of quercetin in cutaneous leishmaniasis. Parasitology, 144(13): 1769–1774.

Srivastava P, Prajapati VK, Rai M and Sundar S (2011). Unusual case of resistance to amphotericin B in visceral leishmaniasis in a region in India where leishmaniasis is not endemic. J Clin Microbiol, 49(8): 3088–3091.

Srivastava S, Mishra J, Gupta AK, Singh A, Shankar P and Singh S (2017). Laboratory confirmed miltefosine resistant cases of visceral leishmaniasis from India. Parasit and Vectors, 10(1): 1–11.

Sujitha, Y.S. and Muzib, Y.I. (2019). Formulation and optimization of quercetin loaded nanosponges topical gel : ex vivo , pharmacodynamic and pharmacokinetic studies. Int J. Appl Pharm, 11(5): 156–165.

Surur AS, Fekadu A, Makonnen E and Hailu A (2020). Challenges and Opportunities for Drug Discovery in Developing Countries: The Example of Cutaneous Leishmaniasis. ACS Med Chem Lett, 11(11): 2058–2062.

Tempone AG, Perez D, Rath S, Vilarinho AL, Mortara RA and de Andrade HF (2004). Targeting Leishmania (L.) chagasi amastigotes through macrophage scavenger receptors: The use of drugs entrapped in liposomes containing phosphatidylserine. Antimicrob Chemother, 54(1): 60–68.

Tiwari B, Pahuja R, Kumar P, Rath SK, Gupta KC and Goyal N (2017). Nanotized curcumin and miltefosine, a potential combination for treatment of experimental visceral leishmaniasis. Antimicrob Agents Chemother, 61(3): 1–13.

Treiger Borborema SE, Schwendener RA, Osso Junior JA, De Andrade Junior HF and Do Nascimento N (2011). Uptake and antileishmanial activity of meglumine antimoniate-containing liposomes in Leishmania (Leishmania) major-infected macrophages. Int J Antimicrob, 38(4): 341–347.

Trinconi CT, Reimão JQ, Coelho AC and Uliana SRB (2016). Efficacy of tamoxifen and miltefosine combined therapy for cutaneous leishmaniasis in the murine model of infection with Leishmania amazonensis. J Antimicrob Chemo, 71(5): 1314–1322.

Valero NNH and Uriarte M (2020). Environmental and socioeconomic risk factors associated with visceral and cutaneous leishmaniasis: a systematic review. Parasitol Res, 119(2): 365–384.

Vannier-Santos M, Martiny A and Souza W (2005). Cell Biology of Leishmania spp.: Invading and Evading. Curr Pharm Des, 8(4): 297–318.

Verma P and Pathak K (2012). Nanosized ethanolic vesicles loaded with econazole nitrate for the treatment of deep fungal infections through topical gel formulation. Nanomed: Nanotechnol Biol Med, 8(4): 489–496.

Want MY, Islammudin M, Chouhan G, Ozbak HA, Hemeg HA, Chattopadhyay AP and Afrin F (2017). Nanoliposomal artemisinin for the treatment of murine visceral leishmaniasis. Int J Nanomedicine, 12: 2189–2204.

Witayaudom P and Klinkesorn U (2017). Effect of surfactant concentration and solidification temperature on the characteristics and stability of nanostructured lipid carrier (NLC) prepared from rambutan (Nephelium lappaceum L.) kernel fat. J Colloid Interface Sci, 505: 1082–1092.

World Health Organization (2012). Research priorities for Chagas disease, human African trypanosomiasis and leishmaniasis. World Health Organization technical report series, (975).

Yasinzai M, Nadhman A and Shahnaz G (2013). Special Focus : Trypanosomatid D iseases Drug resistance in leishmaniasis : current drug-delivery systems and future perspectives. Future Med Chem, 5(15): 1877–1888.

Yuan M, Niu J, Xiao Q, Ya H, Zhang Y, Fan Y, Li L and Li X (2022). Hyaluronan-modified transfersomes based hydrogel for enhanced transdermal delivery of indomethacin. Drug Deliv, 29(1): 1232–1242.

El Zaafarany GM, Awad GAS, Holayel SM and Mortada ND (2010). Role of edge activators and surface charge in developing ultradeformable vesicles with enhanced skin delivery. Int J Pharms, 397(1–2): 164–172.

Zahid F, Batool S, Din FU, Zakir A, Muhammad N, Khan S, Salman O and Khan GM (2022). Antileishmanial Agents Co-loaded in Transfersomes with Enhanced Macrophage Uptake and Reduced Toxicity. AAPS PharmSciTech, 23: 1–18.

Zeb A, Qureshi OS, Kim HS, Cha JH and Kim JK (2016). Improved skin permeation of methotrexate via nanosized ultradeformable liposomes. Int J Nanomedicine, 11: 3813–3824.

Zeb A, Rana I, Choi H, Lee C, Baek S, Lim C, Khan N, Arif ST, Sahar N, Alvi AM, Shah FA, Din FU and Bae O (2020). Potential and Applications of Nanocarriers for Efficient Delivery of Biopharmaceuticals. Pharmaceutics, 2(12): 1184.

Zhang R, Shang L, Jin H, Ma C, Wu Y, Liu Q, Xia Z, Wei F, Zhu XQ and Gao H (2010). In vitro and in vivo antileishmanial efficacy of nitazoxanide against Leishmania donovani. Parasitol Res, 107(2): 475–479.

Turnitin Originality Report

Processed on: 10-Sep-2022 13:45 PKT
ID: 1896448826
Word Count: 9504
Submitted: 1

Nitazoxanide and Quercetin Co-loaded Nanotransfersomal Gel By Sidra Bashir

Similarity Index	Similarity by Source
13%	Internet Sources: 7% Publications: 11% Student Papers: 2%

1% match (publications)
Atif Ullah Khan, Humzah Jamshaid, Fakhar ud Din, Alam Zeb, Gul Majid Khan. "Designing, optimization and characterization of Trifluralin transfersomal gel to passively target cutaneous leishmaniasis", Journal of Pharmaceutical Sciences, 2022

1% match (publications)
Muhammad Waqas Salim, Kanwal Shabbir, Fakhar ud-Din, Abid Mehmood Yousaf, Han-Gon Choi, Gul Majid Khan. "Preparation, In-vitro and In-vivo Evaluation of Rifampicin and Vancomycin Co-loaded Transfersomal Gel for the treatment of Cutaneous Leishmaniasis", Journal of Drug Delivery Science and Technology, 2020

1% match (Internet from 20-Mar-2019)
https://www.tandfonline.com/doi/full/10.1080/10717544.2018.1494222

< 1% match (publications)
Amina Riaz, Naveed Ahmed, Muhammad Ijaz Khan, Ihsan-ul Haq, Asim ur Rehman, Gul Majid Khan. "Formulation of topical NLCs to target macrophages for cutaneous leishmaniasis", Journal of Drug Delivery Science and Technology, 2019

< 1% match (Internet from 28-Dec-2017)
https://www.dovepress.com/getfile.php?fileID=38580

< 1% match (Internet from 29-Mar-2020)
https://www.dovepress.com/front_end/echogenic-pegylated-pei-loaded-microbubble-as-efficient-gene-delivery--peer-reviewed-fulltext-article-IJN

< 1% match (Internet from 02-Mar-2022)
https://www.dovepress.com/getfile.php?fileID=17319

< 1% match (Internet from 01-May-2022)
https://www.researchgate.net/publication/360239429_Infl_uence_of_particle_size_and_ionic_strength_on_the_freeze-thaw_stability_of_emulsions_stabilized_by_whey_protein_isolate-NC-ND_license_httpcreativecommonsorglicensesby-nc-nd40_A_R_T_I_C_L_E_I_N_F_O

< 1% match (Internet from 25-Aug-2022)
https://www.researchgate.net/publication/5361777_Natural_skin_surface_pH_Is_on_average_below_5_which_is_beneficial_for_its_resident_f

< 1% match (publications)
Anam Sajjad Khan, Fakhar ud Din, Zakir Ali, Maryam Bibi, Fatima Zahid, Alam Zeb, Mujeeb-ur-Rehman, Gul Majid Khan. "Development, in vitro and in vivo evaluation of miltefosine loaded nanostructured lipid carriers for the treatment of Cutaneous Leishmaniasis", International Journal of Pharmaceutics, 2021

< 1% match (student papers from 08-Mar-2010)
Submitted to Higher Education Commission Pakistan on 2010-03-08

< 1% match (student papers from 21-Jul-2009)
Submitted to Higher Education Commission Pakistan on 2009-07-21

< 1% match (student papers from 14-Aug-2022)
Submitted to Higher Education Commission Pakistan on 2022-08-14

< 1% match (Internet from 31-Dec-2021)
https://www.hindawi.com/journals/bmri/2021/9968602/

< 1% match (Internet from 25-Aug-2022)
https://www.hindawi.com/journals/tswj/2014/297603/

< 1% match (Internet from 01-Aug-2021)
https://www.hindawi.com/journals/bmri/2021/6619195/

< 1% match (publications)
Sundus Maria, Hafiz Shoaib Sarwar, Muhammad Farhan Sohail, Muhammad Imran et al. "Synthesis and characterization of pre-activated thiolated chitosan nanoparticles for oral delivery of octreotide", Journal of Drug Delivery Science and Technology, 2020

< 1% match (Internet from 23-Oct-2021)
https://link.springer.com/article/10.1007/s13399-019-00399-0?code=232f8f1c-a480-4f32-aab3-c2bdcb42fda0&error=cookies_not_supported

< 1% match (Internet from 25-Mar-2019)
https://link.springer.com/content/pdf/10.1007%2F978-1-4939-1441-8.pdf